NASA-CR-194874

(NASA-CR-194874) SELECTION OF POLYMER BINDERS AND FABRICATION OF SiC FIBER-REINFORCED REACTION-BONDED SILICON NITRIDE MATRIX COMPOSITES Final Report, 10 Dec. 1987 - 24 Feb. 1993 (MIT) 50 p

N94-24223

Unclas

G3/27 0203550

FINAL REPORT

Grant: NAG-3-845 (MIT OSP No. 99857)

Title: SELECTION OF POLYMER BINDERS AND FABRICATION OF SiC FIBER-REINFORCED REACTION-BONDED SILICON NITRIDE MATRIX COMPOSITES

Date: November 1993

Period: 10 December 1987 — 24 February 1993

P.I.: John S. Haggerty

Authors: J. Haggerty, A. Lightfoot, and J. Sigalovsky

Institution: Massachusetts Institute of Technology
Materials Processing Center
Cambridge, MA 02139

TABLE OF CONTENTS

		Page No.
Part I	Effects of Solvent and Polymer Exposures on Nitriding Kinetics of High Purity Si Powders and on Resulting Phase Distributions	2
I.	Introduction	2
II.	Effects of Solvent and Polymer Exposures on Si Surface Chemistry	3
•	Procedures	4
•	Results	4
•	Discussion of FTIR Results	7
III.	Effects of Solvent and Polymeric Exposures on Nitriding Kinetics	7
•	Procedures	8
•	Results	11
•	Discussion of Nitriding Results	12
IV.	X-ray Diffraction Analyses of the Effects of Solvent and Polymeric Exposures on Observed Phases	14
•	Discussion of X-ray Diffraction Results	17
V.	Conclusions and Discussion	18
Part II	Fabrication of Flexural Test Samples	20
I.	Introduction	20
II.	Sample Fabrication	20
III.	Discussion	24
IV.	Conclusions	25
REFERENCES		26
FIGURES		28

PART I EFFECTS OF SOLVENT AND POLYMER EXPOSURES ON NITRIDING KINETICS OF HIGH PURITY Si POWDERS AND ON RESULTING PHASE DISTRIBUTIONS

I. INTRODUCTION

Prior research at MIT explored the effects of various solvents and polymers on the nitriding kinetics and phase distribution of RBSN parts made from high purity SiH_4 derived Si powders.[1-3] These preliminary results showed that the investigated exposures had important consequences on the nitriding rates and extents of conversion.

Continuing studies of the effects which solvent and polymer exposures have on the nitriding kinetics were initiated to provide further guidance for the selection of solvents and polymers, and to determine whether operational restrictions (e.g. time or temperature) should be imposed on burnout and nitriding process steps. Achieving complete conversion to Si_3N_4 was emphasized. The issues that were of principal concern include:

- Achieving complete removal of solvent and polymer at acceptable temperature levels
- Retaining rapid nitriding kinetics
- Minimizing residual Si
- Producing phase-pure Si_3N_4
- Producing uniform parts
- Defining compatible binder systems for fiber and matrix preforms used to make composites

Two types of experiments were undertaken in this research. In the first, the effects of different exposures on the surface chemistries of the Si powders were investigated by diffuse reflectance FTIR analysis (DRIFT-FTIR). In the second, the nitriding kinetics of samples having different exposures were characterized by TGA. The phase distributions resulting in both TGA and furnace nitrided samples were analyzed by X-ray diffraction.

Polymer and solvent combinations employed in these continued experiments were selected primarily based on prior experience with fugitive binders that are candidates for use with high purity reaction bonded silicon nitride. Fugitive polymeric binders were selected which were reported to vaporize in inert atmospheres without leaving residues at temperature levels below the commencement of the nitriding process. The fugitive binders investigated in this continuing research were polystyrene (PS), polymethylmethacrylate (PMMA) and polypropylene (PP). All burn out cleanly according to conventional ceramics processing criteria and are used for injection molding processes with sensitive powders. These binders volatilize at temperatures below levels where the nitridation process begins[4,5] (amorphous Si-N layer begins to form for

T>600°C), avoiding the obvious complexity resulting from both processes occurring simultaneously.

Other fugitive binders which have been evaluated previously with the high purity Si powders include polyethylene (PE), QPAC™ and tetrafluoroethylene/ polystyrene (TFE/PS).[1] Polyethylene based binders are used commonly with ceramic and metal powders; however, the high purity forms used in this study were not soluble in solvents which had been studied previously with respect to their effects on nitriding kinetics. QPAC™ is a commercial binder designed to burn out cleanly in a nitrogen atmosphere.[6] Oxygen contained within the molecule inhibited the nitriding kinetics excessively. The tetrafluoroethylene/ polystyrene (TFE/PS) system has been used extensively by NASA-Lewis in the fabrication of SiC fiber-reinforced RBSN.[7] Previous studies with this binder showed nitriding kinetics were inhibited excessively, and there was evidence of enhanced Si losses by vaporization.

One reactive binder, polysilazane (PZ), was also investigated previously. PZ forms a Si, N and C containing ceramic product upon pyrolysis[8] that is space-filling and evolves lesser amounts of gaseous products which need to escape during burnout. The composition of the final reaction product depends on the composition of the polymer and the pyrolysis atmosphere. In nitriding atmospheres, phase pure Si_3N_4 can be produced. These features should enhance the microstructural quality of the RBSN. Also, the PZ residue may protect the silicon particle surfaces and may offer an alternative reaction site for parallel nucleation of crystalline Si_3N_4. Initial results revealed inhibition of the nitriding kinetics at 1250°C, but complete conversion at 1390°C.[1] Other studies have shown that the Si affects the polymer pyrolysis process.[9] Though complex, reactive binders offer sufficient promise that they should be investigated more extensively.

II. Effects of Solvent and Polymer Exposures on Si Surface Chemistry

In this series of experiments, high purity Si powders were exposed to toluene and xylene solvents, to polymethylmethacrylate (PMMA) dissolved in both solvents, and to polystyrene (PS) dissolved in xylene. These two solvents were selected because they are effective with most candidate polymers, can be dried at low temperatures with minimal residues, and represent acceptable toxicity and fire hazards. PMMA was selected based on its utilization at NASA-Lewis with RBSN/SiC (fiber) ceramic matrix composites. Also, this polymer-solvent combination was not included in previous FTIR studies. The xylene/polystyrene experiments were undertaken because previous MIT research had shown that Si powders processed with this solvent and binder nitrided at the same rates as as-synthesized Si powders.[1]

- Procedures

Powder Si samples were exposed to the pure solvents or to the solvent plus PMMA mixtures in capped glass ampules for varying times, they were dried at either 20 or 150°C, and were characterized by FTIR. All procedures were carried out within a glove box without exposure to air except for a very short time (~5-10 min) during which the samples were loaded into the FTIR.

The toluene/PMMA and xylene/polystyrene samples that were characterized after burnout had different processing histories. The toluene/PMMA samples were made in a glove box atmosphere by the procedures used to make the TGA samples (see following TGA section). The xylene/polystyrene samples were prepared by a spray drying process involving an air exposure. These samples were selected from a group which investigated fabrication of large scale RBSN hypersonic radomes. Pellets of both of these sample types were heated through the binder burnout temperatures (450-480°C) prior to the FTIR analyses which were made on the ground pellets. In contrast, the solvent and solvent plus PMMA samples were only dried as powders.

Identical samples were exposed to the solvents and solvent plus PMMA for approximately 2 hours, 1 week and 2 months. For the PMMA experiments, approximately 0.15 g Si and 0.03 g PMMA were added to 1.5 g solvent. Two drying procedures were used for all sample types; one set was dried for 24 h at 150°C, and the other at room temperature. Dried powder samples were mixed with dry KBr powder using an agate mortar and pestle and the mixtures were placed in the FTIR sample holder cups within the glove box. The samples, contained within the FTIR cups, were placed in polypropylene vials, capped, removed from the glove box and transported to the FTIR apparatus. After insertion into the FTIR chamber (with a short air exposure), the FTIR chamber was continuously purged with N_2 to minimize oxidation during the characterization procedure. Si powder samples (exposed to the glove box atmosphere for 2 hours and 1 week at room temperature, and for 24h at 150°C) that were not exposed to either the solvents or the solvent plus polymer served as references for both drying procedures.

The sample designations and figure numbers for corresponding FTIR patterns are summarized in Table 1 for the toluene, xylene and xylene/PMMA samples. Sample designations include four code elements. For example, the sample F115XPM-2 is made from Batch F115 Si powder, it was exposed to xylene (X), it was bonded with polymethylmethacrylate (PM), and it is the second sample of this type (2).

- Results

Figure 1 summarizes the FTIR spectra of toluene, xylene, PMMA and polystyrene.[10] The results of the FTIR analyses of the solvent and solvent-polymer exposed samples which were exposed to investigated drying cycles are summarized in Figures 2-8. The results for the toluene/PMMA and

xylene/PS samples subjected to binder burnout are reported in Figures 9 and 10. Each figure includes a reference pattern for the as-synthesized Si powder.

The absorption bands summarized in Table 2 have been associated with the indicated bond types on the processed high purity Si powder. In addition, some figures exhibit peaks in the 2300-2400 cm^{-1} range from CO_2 in the FTIR cell resulting from incomplete purging.

Figure 2 exhibits spectral features that are typical of the SiH_4 derived Si powders. Strong absorption features resulting from Si-H bonds are evident at 2080 and 2094 cm^{-1}. An unusually strong feature resulting from Si-O bonding is evident at ~1100 cm^{-1} for this specific batch of Si powder. Independent

Table 1. Summary of exposures and sample designations used for FTIR studies. Numbers in parentheses refer to the corresponding FTIR figure number.

Only Nitrogen Exposure	Toluene Exposure	Xylene Exposure	Xylene & PMMA Exposure	Exposure Time	Drying Temperature (°C)
F115-1 (2)				0	
F115-2 (2)				1 week	20
F115-3 (2)				24 h	150
	F115T-1(3)	F115X-1 (5)	F115XPM-1 (7)	2 hours	20
	F115T-2 (4)	F115X-2 (6)	F115XPM-2 (8)	2 hours	150
	F115T-3 (3)	F115X-3 (5)	F115XPM-3	1 week	20
	F115T-4 (4)	F115X-4 (6)	F115XPM-4 (8)	1 week	150
	F115T-5 (3)	F115X-5 (5)	F115XPM-5 (7)	2 months	20
	F115T-6 (4)	F115X-6 (6)	F115XPM-6 (8)	2 months	150

Table 2. Summary of absorption bands and bond types observed on high purity Si powders.[11-13]

Bond Type:	Si-H	Si-O	Si-N	Si-C	O_X-Si-H	Si-OH	$Si-CH_3$
Wave No. Range: (cm^{-1})	2080-2094	1080-1100	830	800, 790-930	2090-2262	3670-3690	1255-1280

chemical analyses show that the as-synthesized oxygen level is approximately 160 ppm, or less than 4% of a monolayer. Figure 2 shows that no significant change in surface chemistry occurred with exposing open powders to the glove box atmosphere for 1-week at room temperature. Figure 2 also shows that an additional 24 h exposure to the glove box atmosphere at 150°C resulted in an increase of the oxygen band and a slight decrease in the 2100 cm^{-1} Si-H band. These results show that neither simulated drying cycle caused any significant effect on the surface chemistries of Si powders which had not been exposed to solvents or to solvent plus polymer.

Figures 3-8 summarize the effects of solvent and polymer exposures for different times and different drying conditions.

Minimal exposures to solvents and polymers (2-hours and room temperature drying) caused obvious changes in samples F115T-1, F115X-1 and F115XPM-1 (Figures 3, 5 and 7). In all three sample types, the intensities of the Si-O peaks at 1100 cm^{-1} increased relative to the Si-H peak at 2100 cm^{-1}. All three also developed both more pronounced and new absorption features between 1000 and 2000 cm^{-1}; in particular, the PMMA exposed sample (F115XPM-1) exhibited features resulting from the PMMA. Increasing the drying temperature to 150°C for the 2-hour exposed samples (F115T-2, F115X-2 and F115XPM-2) caused further expansion of the Si-O peaks and contraction of the Si-H peaks as shown in Figures 4, 6 and 8 respectively. Samples exposed for 2 months and dried at room temperature (F115T-5, F115X-5 and F115XPM-5) exhibited the same expansion of the Si-O peaks and contraction of the Si-H peaks as is shown in Figures 3, 5 and 7 respectively. The samples exposed for 2 months and dried at room temperature appeared approximately equivalent to those exposed for 2-hours and dried at 150°C. The most severe conditions (2-month exposure and 150°C drying) caused samples F115T-6, F115X-6 and F115XPM-6 to lose most evidence of Si-H bonding and to develop very pronounced Si-O bonding as is shown by Figures 4, 6 and 8 respectively. One week exposures exhibited absorption results which were intermediate between those observed for the 2-hour and 2-month exposures having the same drying conditions (Figures 7, 8, 13, 14, and 19).

The PMMA exposed samples (F115XPM-1, F115XPM-2, F115XPM-3, F115XPM-4, F115XPM-5 and F115XPM-6) all exhibit spectral features that are characteristic of PMMA (compare Figures 1 with 7 and 8). Many of these PMMA peaks obscure the Si-O peaks in the shorter, lower temperature exposed Si samples. The sample exposed for 2 months (F115XPM-6) exhibited significant decreases in some of the smaller PMMA peaks, but the characteristic carbonyl peak at 1730 cm^{-1} remained predominant. The patterns exhibit less Si-H bonding than the corresponding xylene patterns.

The FTIR results for the toluene/PMMA and xylene/polystyrene samples after binder burnout cycles are given in Figures 9 and 10. Compared with the as-synthesized Si powder, both powders exhibited increased Si-O bonding at 1100 cm^{-1} and reduced Si-H bonding at 2100 cm^{-1}. Both exhibit O_x-Si-H bonding at 2090-2262 cm^{-1}. The toluene/PMMA spectrum exhibits H_2O bands at 1400-1800 and 3600-3900 cm^{-1} as well as CO_2 bands at 2300-2400 cm^{-1} which both result from incomplete purging of the sample chamber. The Si-CH_3 band at 1255-1280 cm^{-1} is strong in the toluene/PMMA sample but is weak in the xylene/PS sample. Previously, we had associated this type of residual carbon bonding with rapid nitriding kinetics.[1]

- Discussion of FTIR Results

These results clearly indicate that toluene and xylene modify the surface chemistries of the high purity Si powders much more than occurs after simply exposing the powders to a N_2 atmosphere for prolonged storage or to the conditions used for drying. Increasing exposure times and temperatures cause progressively greater changes, thus both should be minimized. Vacuum drying and minimizing the period between the time the powders are dispersed to the beginning of nitridation are both obvious suggested modifications based on these findings.

The sources of the oxygen have not been identified. However, it is likely that trace levels of water in the solvents (0.01% for toluene and 0.016% for xylene) were responsible for much of the observed oxidation. The glove box contained house N_2 which has 10-100 ppm O_2; this oxygen probably contributed to the increased oxidation during 150°C drying.

With heating through binder burnout temperatures, much of the protective Si-H bonding is lost, making the powders susceptible to oxidation. Consequently, both investigated samples exhibited much increased Si-O types of bonds. These results indicate that nitriding must be done without exposing the samples to air after being exposed to burnout temperatures in excess of ~450°C.

III. Effects of Solvent and Polymeric Exposures on Nitriding Kinetics

The effects of candidate solvent and binder combinations on the nitriding kinetics of the SiH_4 derived Si powders have been investigated. The polymers that were studied included polystyrene, polymethylmethacrylate and polypropylene. Solvents included toluene and xylene; also, dry polymers were used to isolate the combined effects of the solvent and polymer. As-synthesized Si powder was used as a reference.

This series of experiments was designed to provide preliminary descriptions of the effects these polymers and solvents had on nitriding kinetics and to explore the most obvious effects of manipulated process variables. More detailed nitriding experiments and characterizations are required for interpretation of nitriding mechanisms and for process optimization.

Polystyrene was investigated since this polymer has been selected as the binder in the first series of test samples for the hypersonic radome application. This selection was based on observed nitriding kinetics and room temperature dielectric properties. Polymethylmethacrylate was selected because it has been used successfully at NASA-Lewis for fabricating RBSN/SiC (fiber) composites from polymer bonded preforms. Polypropylene was selected because literature citations indicated it volatilized completely in inert atmospheres without leaving residues. Specific solvent-polymer combinations were based on solubilities. Toluene was used with PMMA in these series of experiments because xylene proved to be a poor solvent at room temperature in the FTIR studies. Sample designations and firing schedules are summarized in Table 3.

- Procedures

Pellet samples (1.2 cm diameter x 0.1-0.2 cm thick) were processed with minimal exposure to air and other contaminants. Pellets were pressed at room temperature at a pressure of 56.2 MPa (8,150 psi) from dried powders in a single action press.

Individual processing histories varied for the different solvent and polymer types. The F121XPS series of polystyrene bonded samples were made from powders that were spray dried at Raytheon. The dry PMMA sample (F121PM type) was made from Si and PMMA powders that were physically mixed for 3 minutes in a vial. The toluene processed PMMA samples (F121TPM type) were prepared by dissolving the PMMA in hot toluene, adding the Si powder while mixing for 1 minute, and then drying the mixture in a watch glass within the glove box; the dried powder was ground by hand before pressing. Dry processed polypropylene samples (F121PP-1 type) were made from dry mixed polypropylene and Si powders similar to the dry PMMA samples. The xylene dissolved polypropylene samples (F121XPP-1 to -3) were made by dissolving the polypropylene in hot xylene, mixing in the Si powders, drying the mixtures in a watch glass within a glove box, and grinding the dried powders.

After the powder for each pellet type was prepared, 355 mg of dried powder was placed into a vial. The closed vial was then transferred to the press where the powder was introduced to the die in an air atmosphere. With losses, the process yielded 350 mg pellets. When the pellet was removed from the die, it was weighed, and carried to the TGA apparatus. Gloves were always worn when handling the samples and the boat.

Pressed pellets were immediately transferred to a Netzsch Model STA 429 TGA/DTA apparatus where they were loaded and evacuated. The entire air exposure of the pressed samples lasted between 30 and 60 minutes. After establishing a vacuum to verify hermeticity, the samples were subjected to the heating schedules summarized in Table 3. UHP N_2 (nominal 10 ppm O_2) was used for nitriding.

Table 3. Designations and processing histories for samples used in TGA studies. The indicated polymer contents are weight percent polymer based on the Si + polymer content.

Sample	Solvent Binder	Solvent Removal	Binder Burnout	Heat to 1st Hold	Heat to 2nd Hold	Nitriding Hold
Pure Powder						
F121-1	none	vacuum 20°C/m 140°C 1h hold	none	N_2 100°/m to 1255°	none	until stable
Polystyrene						
F121XPS-1	xylene 5% PS	vacuum 20°C/m 140°	N_2 20°/m to 330° 2°/m to 540°	N_2 100°/m 1254°	none	until stable
F121XPS-2	xylene 5% PS	vacuum 20°C/m 120°	N_2 20°/m to 120°	N_2 2°/m to 1254° 4h hold	N_2 0.5°/m to1395°	10h
F121XPS-3	xylene 5% PS	vacuum 20°C/m 132°	N_2 20°/m to 132° 2°/m to 540°	N_2 100°/m to 1255° 4h hold	N_2 0.5°/m to 1396°	10h
Polymethylmethacrylate						
F121PM-1	none 10% PMMA	vacuum 20°C/m 119°	N_2 20°/m to 280° 2°/m to 500°	N_2 100°/m 1254°	none	until stable
F121TPM-1	toluene 10% PMMA	vacuum 20°C/m 108°	N_2 20°/m to 160° 2°/m to 500°	N_2 100°/m 1256°	none	until stable
F121TPM-2	toluene 10% PMMA	vacuum 20°C/m 110°	N_2 20°/m to 160° 2°/m to 500°	N_2 100°/m to 1254° 4h hold	N_2 0.5°/m to 1394°	10h
Polypropylene						
F121PP-1	none 10% PP	vacuum 20°C/m 109°	N_2 20°/m to 280° 2°/m to 560°	N_2 100°/m to 1256°	none	until stable
F121XPP-1	xylene 10% PP	vacuum 20°C/m 125°	N_2 20°/m to 340° 1°/m to 560°	N_2 100°/m to 1255°	none	until stable
F121XPP-2	xylene 10% PP	vacuum 20°C/m 125°	N_2 20°/m to 340° 1°/m to 560°	N_2 100°/m to 1157°	none	until stable
F121XPP-3	xylene 10% PP	vacuum 20°C/m 124°	N_2 20°/m to 340° 1°/m to 560°	N_2 100°/m to 1205° 4h hold	N_2 0.5°/m to 1396°	10h

Table 4. Summary of TGA Si-nitriding results

Sample Type & Designation	Binder & Solvent	Max Nitriding Temp	Initial Wt. (g)	Measured Binder Loss (g)	Expected Binder Loss (g)	% Expected Binder Loss	Max Binder Loss Rate (mg/min)	Temp at Max Binder Loss Rate (°C)	Burnout Temperature Range (°C)
Pure Si Powder									
F121-1	None	1250	0.3332	0.0000	0.0000	-	0.000	-	-
Polystyrene + Si									
F121XPS-1	10%PS+Xylene	1250	0.3429	0.0144	0.0171	83.9	0.235	350	210-465
F121XPS-2	10%PS+Xylene	1400	0.3441	0.0145	0.0172	84.2	0.283	357	170-475
F121XPS-3	10%PS+Xylene	1400	0.3514	0.0144	0.0176	81.7	0.265	365	215-470
Polymethylmethacrylate + Si									
F121PM-1	10% PMMA, dry	1250	0.2740	0.0337	0.0280	120.6	1.200	340	230-415
F121TPM-1	10%PMMA+Toluene	1250	0.3506	0.0305	0.0353	86.4	0.764	330	220-420
F121TPM-2	10%PMMA+Toluene	1400	0.3616	0.0325	0.0364	89.4	0.795	335	275-430
Polypropylene + Si									
F121PP-1	10%PP, dry	1250	0.3400	0.0348	0.0347	100.5	1.920	420	345-485
F121XPP-1	10%PP+Xylene	1250	0.3523	0.0337	0.0355	94.9	0.908	420	305-440
F121XPP-2	10%PP+Xylene	1150	0.3489	0.0376	0.0351	107.2	0.990	420	365-450
F121XPP-3	10%PP+Xylene	1400	0.3504	0.0416	0.0352	118.0	1.240	430	335-430

Sample Type & Designation	Initial Si Wt (g)	Final Nitrided Wt (g)	Nitriding Weight Gain (g)	% Conversion	Bulk Density (g/cc)	Theoretical Density (g/cc)	% Theoretical Density	Induction Time (min)	Max Wt Gain Rate (%theo/min)
Pure Si Powder									
F121-1	0.3332	0.5549	0.2217	100.06	2.085	3.18	65.56	-2.10	21.66
Polystyrene + Si									
F121XPS-1	0.3285	0.5234	0.1949	89.20	1.936	3.10	62.39	12.50	12.30
F121XPS-2	0.3296	0.5440	0.2144	97.80	2.021	3.16	63.87	7.40	8.52
F121XPS-3	0.3370	0.5554	0.2184	97.42	1.983	3.16	62.71	15.00	8.51
Polymethylmethacrylate + Si									
F121PM-1	0.2403	0.3192	0.0789	49.37	1.387	2.79	49.69	16.50	3.34
F121TPM-1	0.3201	0.3872	0.0671	31.50	1.435	2.64	54.43	12.90	1.36
F121TPM-2	0.3291	0.5375	0.2084	95.22	1.975	3.15	62.75	13.75	1.04
Polypropylene + Si									
F121PP-1	0.3052	0.4805	0.1753	86.40	-	3.08	-	0.00	56.69
F121XPP-1	0.3186	0.5001	0.1815	85.64	1.829	3.08	59.43	7.50	21.01
F121XPP-2	0.3113	0.4736	0.1623	78.41	1.781	3.02	58.92	268.00	0.29
F121XPP-3	0.3088	0.5074	0.1986	96.69	1.826	3.16	57.84	39.75	2.48

- Results

The results of the TGA experiments are summarized in Figures 11-21, and results are analyzed in Table 4. Note that this text refers to nominal temperature set points while Tables 3 and 4 report actually measured temperatures.

The TGA curves (except F121XPS-2) include the initial heating used for drying and binder burnout. These initial portions of the curves exhibit weight losses. The zero values on the "percent nitrided" axes were defined based on the Si weights. The zero values on the time axes were defined by the time the temperature reached a level equal to 10°C less than the initial nitriding temperature. This time approximates the beginning of the induction period.

The following definitions are provided to avoid ambiguities about terms used in Table 4.

Initial Weight: pellet weight immediately after pressing including the binder and solvent residuals.

Binder Loss: calculated by adding together the observed weight losses during the vacuum heating and the binder burnout periods.

Expected Binder Loss: amount of binder expected to be contained by the parts based on batch formulations.

Percent Expected Binder Loss: calculated from the quotients of the actual and expected binder loss values.

Maximum Binder Loss Rate: calculated from the maximum instantaneous slopes of the weight-time curves during the binder burnout periods.

Silicon Weight: calculated by subtracting the binder losses from the initial pellet weights.

Final Weight: determined by weighing the nitrided pellets immediately after they were removed from the TGA furnace.

Density: calculated using the final weights, diameters, and thicknesses.

Percent Conversion: estimates based on weight changes were calculated using the following formula: Percent conversion = [(final weight-silicon weight) / (0.665 x silicon weight)] x 100.

Nitrogen Weight Gain: calculated by subtracting silicon weights from final weights.

Theoretical Density: volume weighted average densities calculated based on the percent conversion and the theoretical densities of Si and Si_3N_4 (2.33 and 3.18 respectively).

Percent Theoretical Density: calculated based on the quotients of the actual and theoretical densities.

Induction Time: calculated from the differences between the ends of the induction periods and the times the furnace reached a level 10°C below the final holding temperatures. The ends of the induction periods were defined to be the times at which the weight-time curves changed from being either concave downward or linear to being concave upward at the beginnings of the fast reactions. Because of the definition, both positive and negative times are possible. The "zero-time" values reported in the figures correspond to the beginnings of the induction periods.

Maximum Weight Gain Rate: calculated from the maximum slopes of the weight-time curves during the fast reaction periods normalized to the expected nitrogen weight gains for 100% conversion.

- Discussion of Nitriding Results

The nitriding kinetics exhibited by the dry processed Si powder used as a reference (Figure 11, sample F121-1) were similar to previous results with other batches of Si powder. Virtually complete nitridation was achieved within less than 10 minutes of reaching 1250°C at a heating rate of 100°C/m. The induction period occurs during heating, so it is reported as a negative value in Table 4.

While dramatic, the heating rates and reaction rates observed with the dry Si powders are impractical for larger parts employing binders and solvents. Slower heating is required until the parts are dried and the binders have burned out to avoid fracturing the parts. Slower reaction rates are required to prevent overheating during the highly exothermic reactions.

Three polystyrene bonded samples were nitrided. The first employed the same heating schedule (100°C/m) to the 1250°C nitriding temperature as was used for the pure Si reference sample after binder burnout at 470°C (Figure 12, sample F121XPS-1). As observed previously,[1] exposure to xylene and polystyrene caused the induction period to be extended, but the fast reaction rate was comparable to the pure Si reference once it began. At 1250°C, the fast reaction terminated with approximately 7-10% unreacted Si. The second and third polystyrene bonded samples included second heating steps to 1395°C at 0.5°C/m after 4 hour holds at 1250°C. One sample (Figure 13, sample F121XPS-2) employed the slow heating rate to 1250°C used for larger furnace nitrided samples (2°C/m) and the other (Figure 14, sample F121XPS-3) employed the rapid (100°C/m) rate normally used in the TGA. The second heating step to 1395°C induced nitridation of most of the Si remaining after the 4 hour holds at 1250°C. For both, the second high temperature reaction commenced slowly at approximately 1300-1310°C, became very rapid at ~1390°C, and appeared to terminate when the temperature stabilized at

1395°C. Although the sample heated at the slower rate exhibited a slightly lower conversion at 1250°C (85 vs. 89%), it resumed a slow, progressive reaction rate sooner during the second heating in the 1300-1390°C range so that the final jump involved less Si. Heating to 1395°C induced virtually complete conversion to Si_3N_4 in the xylene and polystyrene exposed samples.

Three polymethylmethacrylate bonded samples were nitrided in the TGA. All three employed the same heating rate (100°C/m) that was used for the Si reference to 1250°C after burnout had been completed at 425°C. The effects of the solvent and binder were isolated in the first and second samples (Figures 15 and 16, samples F121PM-1 and F121TPM-1 respectively) which were not heated higher than 1250°C. The third added a second heating step to 1395°C after a 4-hour hold at 1250°C for the toluene and PMMA exposed sample (Figure 17, sample F121TPM-2).

These results show that the PMMA alone dramatically suppressed the conversion to Si_3N_4 at 1250°C, and that the introduction of toluene inhibited it even further. In both cases, premature termination of the fast reaction period, rather than extension of the induction period or slow reaction rate, was responsible for the low levels of conversion. All three exhibited a small, but finite, reaction rate during the hold at 1250°C after the fast reaction had terminated. As soon as the temperature was raised above 1250°C, Figure 17 shows that the toluene and PMMA exposed sample began to convert to Si_3N_4. The rate of conversion increased progressively until reaching a constant value at approximately 1310-1320°C; the reaction terminated abruptly at 1395°C when the maximum temperature was reached.

As observed for the polystyrene bonded samples, the polymethylmethacrylate bonded samples converted nearly to completion with heating to 1395°C. Residual Si levels are estimated to be nominally 5%. Longer hold times and higher nitriding temperatures will probably result in full conversion of both types of samples. The PMMA bonded samples exhibited a much more gradual conversion during the second heating step than was observed with PS. This feature should make nitridation much more controllable with a PMMA binder.

Four polypropylene bonded samples were studied. The first two were intended to isolate the effects of the xylene solvent in polypropylene bonded samples that were heated to 1250°C at 100°C/m after binder burnout had been completed (Figures 18 and 19, samples F121PP-1 and F121XPP-1 respectively). The xylene did not have a major influence on nitriding characteristics. The xylene and polypropylene bonded sample exhibited essentially the same characteristics as the corresponding polystyrene bonded sample. After a slightly extended induction period, it nitrided at rates comparable to the Si references until the fast reactions terminated at approximately 85% conversion. Because the fast reaction rates were excessive at 1250°C, the nitriding temperature was lowered to 1150°C for sample F121XPP-2 (Figure 20). This

sample exhibited a prolonged induction period (268 min), but then began to convert at acceptable rates. This nitriding experiment was terminated at ~90% conversion; however, the nitriding reaction was still proceeding. The fourth polypropylene bonded sample (Figure 21, sample F121XPP-3) was nitrided with a schedule that included a second higher temperature step. Sample F121XPP-3 (Figure 33) was heated first to an intermediate temperature (1200°C) to shorten the induction period with respect to the 1150°C experiment; after a 4-hour hold it was heated at 0.5°C/m to 1395°C to complete the reaction during a 10-hour hold. Similar to the PMMA sample F121TPM-2 (Figure 17), this sample began to nitride as soon as the temperature was raised above the 1250°C hold. Nitridation rates began to increase significantly at approximately 1320°C, and became extremely rapid at ~1370°C. As with the PS and PMMA bonded samples, the initial level of nitridation (80-85%) at 1250°C increased to >95% with the second heating step to 1390°C.

The two-step nitriding experiments demonstrate a result that is very important for achieving complete nitridation. Although we have suggested several possible explanations for the termination of the fast reaction periods, we have not defined which is responsible. The resumption of the reactions for T>1250°C strongly suggests that the reactions do not terminate because mass transport (Si or N_2) is blocked by the Si_3N_4 reaction product, either on the local scale of the Si particles or on the macroscale of the interconnected pore structure within the samples. Diffusivities in crystalline Si_3N_4 are simply too low in the 1250-1390°C range to permit observed reaction rates. It is also probable that the barrier operates only on the scale of the Si particles since transport path lengths are too long to permit condensed phase diffusion throughout the samples at required rates. These results indicate that termination of the fast reaction periods probably results from a localized condensed phase that blocks the transport of N_2 or Si in the proximity of the residual Si particles and the grains of the Si_3N_4 reaction product. They further suggest either that diffusivities in the blocking phase increase rapidly for 1300<T<1390°C, or that its morphology changes in this temperature range thereby permitting the reaction to proceed. The similarity of the polystyrene, polymethylmethacrylate, and polypropylene elevated temperature results suggests that the same blocking material forms for all three polymers, but does not for the pure Si powder.

IV. X-RAY DIFFRACTION ANALYSES OF THE EFFECTS OF SOLVENT AND POLYMERIC EXPOSURES ON OBSERVED PHASES

Representative TGA samples (Tables 3 and 4) were analyzed by quantitative X-ray diffraction as a function of distance from their exterior as-nitrided surfaces. The phases that were analyzed were Si, α-Si_3N_4, β-Si_3N_4, and SiC. The results of the calculated percent conversions to Si_3N_4 are summarized in Figures 22 and 23 for dry processed pure Si (F121-1), polystyrene exposed Si (F119XPS-2 and F121XPS-1), polymethylmethacrylate exposed Si (F121PM-1 and F121TPM-1) and polypropylene exposed Si (F121XPP-1, -2 and -3).

With the exception of sample F121XPP-3, the conversions defined by weight gain (Table 4) and by X-ray were in excellent agreement. For sample F121XPP-3, weight changes indicated 96.69% conversion, while X-ray analyses indicated complete conversion to Si_3N_4 throughout the sample. With the uncertainties resulting from the relatively high weight losses during binder burnout, the X-ray results should be considered the more accurate measure of residual Si, which is less than 0.5% in this sample.

Both the percent conversion results, shown in Figures 22 and 23, and the α-Si_3N_4 to β-Si_3N_4 ratio results in Figures 24 and 25 indicate the presence of gradients in some of the samples. As has been observed previously for these high purity Si powders, conversion to Si_3N_4 tends to be inhibited near the exterior surfaces of the samples because of effects resulting from oxygen contamination. This effect is greatest in the dry processed Si powders having no prior solvent or polymer exposures, and can be minimal when Si powders are exposed to polymers and solvents. For the systems studied, conversion gradients were limited to depths less than 200 μm.

The α-Si_3N_4 to β-Si_3N_4 ratios reported in Figures 24 and 25 indicate the effects polymer and solvent exposures have on Si_3N_4 nucleation since we have shown that nuclei form only during a very short interval of time at the end of the induction period, and that measured α/β ratios are independent of the extent of conversion. Selected area TEM diffraction analyses of the high purity RBSN has shown that α-Si_3N_4 nucleates on 3 Si planes and that β-Si_3N_4 nucleates on only one.[14] With equal probability of nucleation on both types of planes, the α/β ratio should be 3 to 4. The pure Si sample in Figure 24 exhibits the lowest, nearly ideal α/β ratio, indicating that β-Si_3N_4 nucleation is not inhibited by accidently introduced contaminates. The polypropylene and polystyrene plus solvent exposed samples exhibit elevated α/β ratios, indicating their suppressing effects on β-Si_3N_4 nucleation. In contrast, the polymethyl-methacrylate exposed samples (with and without solvent) exhibited lower α/β ratios and retarded reaction kinetics, indicating that nucleation of both phases is suppressed. The 1150°C polypropylene sample exhibited a higher α/β ratio than the two polypropylene samples that were subjected to higher initial nitriding temperatures. This may be a simple temperature effect as was observed by Sheldon[14] with unexposed high purity Si powder, or it may result from oxygen contamination that occurred during the prolonged induction period at 1150°C. The α/β gradients exhibited by the polymer exposed samples are opposite to those normally observed for unexposed high purity Si powders using ungettered UHP N_2.[15] Oxygen contamination near exterior surfaces normally causes elevated α/β ratios near the surfaces of high purity Si samples.[14]

All three polymers reduce the extents of conversion to Si_3N_4 at 1250°C relative to that achieved (>98%) with pure, dry processed Si powders (sample F121-1). Within the interiors of the samples that were nitrided at this temperature,

polystyrene achieved the highest conversion (~85-90%), polypropylene was intermediate (~80-85%), and polymethylmethacrylate was the lowest (~25-30%). With longer exposures to higher nitriding temperatures (e.g., 1390°C for 10 hours), representative interiors of polystyrene and polypropylene sample types have exhibited complete conversion (>99%) to Si_3N_4.

Even though the 1390°C-10h nitridation schedule can result in complete conversion, it does not always achieve this goal. Dry processed 1-inch diameter 1/4-inch thick samples nitrided in a horizontal tube furnace for up to 250 hours exhibited lower levels of conversion than similar 1/2-inch diameter 1/8-inch thick TGA samples that were nitrided even with shorter periods and lower temperatures. Figures 26 and 27 summarize the X-ray diffraction analyses of percent conversions and α/β ratios as a function of distance from bottom and top exterior surfaces of the as-nitrided samples. Top and bottom surfaces were similar for all samples. Extent of conversion and α/β gradients were more evident in the 10h samples than in those nitrided for 50 and 250 hours. These X-ray results demonstrate that the reaction proceeds quite uniformly throughout the samples in terms of both residual Si levels and α/β ratios. This result indicates that the failure to achieve complete nitridation in the larger diameter samples made without exposure to polymers or solvents results from factors that operate on the very localized scale of the Si particles rather than macroscopic transport through the pore structure.

X-ray diffraction line broadening analysis was used to determine the grain size of the residual Si in samples made from dry processed Si powders, and those made with polystyrene and xylene exposures. The results are summarized in Table 5. The initial grain size was based on TEM analysis of as-synthesized Si powders which have shown that most particles are single crystals.[16] Thus, the initial Si grain size is approximately equal to the particle size. Based on measured green densities and particle sizes, the as-pressed Si pellets contain approximately 7×10^{13} particles per cubic centimeter. Line broadening analysis shows that the Si grain sizes in all of the nitrided samples are 510 to 547 Å. Since Si grain size refinement is unlikely to result from the nitriding schedule, these dimensions correspond to the diameters of the residual Si particles. These diameters combined with the volume fractions of unreacted Si in the samples permits calculation of the number of residual Si particles per cubic centimeter of Si_3N_4. Generally, the values given in the fourth column agree within an order of magnitude with the initial Si packing density. An independent check of the results is provided by comparing the volume percentages that the final Si particles constitute of the original Si particles. Again, within an order of magnitude, the volume percentages of free Si derived by the two estimates agree with one another. These results are a further corroboration that complete conversion is blocked by factors operating on the scale of the Si particles.

Table 5. Residual Si grain size analysis by X-ray diffraction line broadening

Initial Si grain size = 2500Å
Particles/volume = 7×10^{13} cm^{-3}

Nitrided Sample	Ave. Residual Si Grain Size (Å)	Vol. % Free Si	No. Si Particles cm^{-3}	$(D_f/D_o)^3$ x 100 (%)
Virgin-dry				
1390°C-10h	523	1.4	1.8×10^{14}	0.9
1390°C-50h	523	2.4	3.0×10^{14}	0.9
1390°C-250h	514	4.4	5.8×10^{14}	0.9
PS-xylene				
1390°C-10h (front)	547	2.5	2.7×10^{14}	1.0
1390°C-10h (center)	510	3.1	4.3×10^{14}	0.9

When greater masses (either larger numbers of 1/2" samples or samples with larger dimensions) of polystyrene bonded samples were nitrided in a horizontal tube furnace, it was noted that brown-black condensate formed on the cooler regions of the furnace, and that the RBSN samples frequently were darker than the light tan color of the fully nitrided samples. In contrast to polystyrene bonded samples that were nitrided in the TGA apparatus, several indications suggested that the samples were exposed to carbon residue during nitridation in the tube furnace. Figure 28 shows the results of quantitative X-ray analysis as a function of depth from the exterior surface for a sample that was located close to the boundary of the brown-black discoloration in the tube furnace. This sample contained up to 30% SiC near its exterior surface. This result shows that carbon traces, resulting from incomplete removal of the polystyrene binder, remain somewhere within the tube furnace after burnout and that they can react with the Si during the nitriding process. The gradient from the exterior surface indicates that the carbon was successfully removed from the sample during burnout, but was then reintroduced to the sample after further heating evidently because the volatilization products were not removed from the furnace.

- Discussion of X-ray Diffraction Results

For virtually all of the samples, the percentage conversion values derived by weight change and X-ray techniques agreed within 1-2%. Generally, the weight change values were intermediate within the gradient range defined by profiling the samples. This corroboration is important since it shows that the accounting of weight changes during drying, burnout and nitriding steps is being carried out with a high level of precision. This agreement will permit future experimental campaigns to be conducted with minimal duplication of these determinations.

The X-ray diffraction profiles of the samples showed that both the conversion and the α/β gradients, which are particularly evident in virgin dry-processed samples nitrided at minimum temperatures, are virtually absent in polystyrene

and polypropylene bonded samples nitrided for 10 hours at 1390°C. Compositional uniformity can be achieved using the employed processing techniques.

The X-ray diffraction results confirmed that many of the recent furnace processed samples did not nitride as extensively as the TGA samples that were used to select initial process conditions. Line broadening analysis indicated that residual Si was distributed uniformly throughout these samples in accordance with a shrinking core reaction model. Other observations also suggested that the nitriding reactions were blocked from proceeding to completion by factors which operated on the scale of the Si particles; blockage probably was not caused by protective Si_3N_4 layers on the Si particles. Further characterization of these samples as well as prior samples is required to interpret this finding because it contradicts our previous interpretations about the nature of the unreacted Si. Extensive TEM characterization of earlier samples revealed only a few, widely separated essentially unreacted Si grains in the RBSN samples.[16] These earlier results indicated that incomplete conversion resulted from isolated particles failing to react, most likely because the pore structure closed prematurely, precluding transport of N_2 to the particles. The distinction is important because different strategies are needed to insure complete conversion for the two cases.

The X-ray results also revealed an important difference between the TGA samples and the furnace fired samples. For the first time, the furnace fired samples confirmed problems associated with the binder that were suspected on the basis of discolorations of the furnace and the RBSN samples. In one case where a Si sample was positioned near a condensation line within the horizontal tube furnace, the RBSN sample contained high levels of SiC. The Si gradient in the sample indicated that the binder had been successfully removed from the sample, but that it apparently condensed within the furnace and was transported back to the sample where it reacted when the temperature level was increased from the burnout level to the nitriding level.

V. Conclusions and Discussion

These experiments indicate that exposures to polymers and solvents have direct effects on the surface chemistries of the high purity Si powders, and that these exposures influence the nature of the nitriding kinetics.

Beyond the emergence of the polymer absorption features, gradual loss of Si-H bonding and progressive increase of the Si-O types of bonds were the most obvious consequences of interactions with the Si particles. These changes in both bond types have previously been correlated with retarded and incomplete nitridation. The progressive nature of these changes very strongly suggests that these exposures must be optimized and defined in establishing a fully controlled process. This optimization will minimize the drying temperatures and times, probably by conducting them in vacuum.

As had been observed previously, exposures to the investigated solvents, binders and atmospheres generally affected the induction periods, the magnitude of the fast reaction rates, and the extent of the reactions at the termination of the fast reaction periods. Both polystyrene (the polymer selected for the first series of evaluation experiments) and polypropylene caused a slight extension of the induction period, but had little effect on the fast reaction rate or the extent of conversion at 1250°C. Residues appear to offset the inhibiting effects of the changes in surface chemistry. Polymethylmethacrylate effectively blocked the reaction at 1250°C. Inclusion of higher nitriding temperatures showed that the Si remaining after 4 hours at 1250°C could be largely converted to RBSN for Si powders having all prior exposures.

Although results cannot be unequivocally isolated because several experimental parameters were manipulated simultaneously, evidence suggests that excessive nitriding rates in the 1250°C range inhibited complete conversion at the higher temperatures. The effect of the highly exothermic nitriding reaction is exacerbated at the 1250°C level with higher masses of Si samples and with larger sample dimensions. Optimum process conditions must control the initial reaction rates within limits defined by the final level of conversion, rather than maximize the rates as has been done in the past. Results with varied process conditions clearly show that simple manipulations of heating rates and hold temperatures will permit the reaction rates to be slowed down without adversely affecting the final level of conversion. Diluting the gas stream with He, or other inert gas, as well as introducing N_2 demand control strategies, are other means of controlling the exothermic reactions.

Consequences of polymer residues in the horizontal tube furnace were qualitatively evident in the furnace and the samples. Observed SiC gradients indicate that the polymers were successfully removed from the samples during burnout, but that the volatilization products were not removed from the furnace. Evidently, the carbon residues were transported back to the samples at higher temperature levels. Improved removal of the products will be explored through modified gas flow patterns within the furnace and the use of vacuum during burnout.

Overall, these results continue to indicate that complete nitridation of the high purity Si powders can be accomplished using solvents, binders, short air exposures, and handling procedures needed to make large shapes. As should be expected, the results show that process details must be defined and carefully controlled to achieve the unusually high qualities needed for reliable high temperature structural materials. The results indicate that there is no obvious reason why objectives cannot be met using the polystyrene/xylene system selected for initial shaping experiments. They also show that other polymers and solvents remain viable choices.

PART II. FABRICATION OF FLEXURAL TEST SAMPLES

I. INTRODUCTION

The final portion of this program applied the nitriding kinetics information learned from 1/2" diameter TGA samples to the production of 49 mm x 6 mm x 4 mm flexural test samples. Eight of these bars were submitted to NASA-Lewis for high temperature tests.

These monolithic bars were formed and nitrided in a manner consistent with combining the silicon powders with SiC fiber reinforcements. Nominal procedures are described below, followed by a presentation of resulting bar characteristics and a discussion of problems which were addressed in scaling from the small TGA samples to the bar samples. Physical characteristics of all bars are summarized in Tables 6 and 7.

II. SAMPLE FABRICATION

Nominal 0.25 μm diameter laser-synthesized Si powders were spray-dried from a polystyrene/xylene solution in preparation for dry pressing. The only air exposure during fabrication of most samples occurred during powder transfers before and after spray drying. The spray dried powder contained 5 wt% polystyrene. The powders were die pressed into bar shapes, then bagged for isopressing in a N_2 atmosphere glove box. A rectangular steel die was charged with powder and uniaxially pressed at room temperature to 70 MPa (10 ksi). The bars were wrapped in 76 μm (0.003 inch) Teflon,™ vacuum sealed in 100 μm (0.004 inch) polyethylene, and vacuum sealed in rubber bags prior to 110°C, 276 MPa (40 ksi) isopressing. After isopressing, bars were returned to the glove box for unwrapping, measurement, and loading into the portable, hermetic nitriding furnace tube.

Binder removal and nitriding were carried out consecutively in the same Al_2O_3 furnace in an atmosphere of UHP N_2 flowing at 75 sccm. Initially, nitriding schedules varied until TGA optimization data became available. Schedules used for all bars are detailed in Table 8. The optimized schedule (E), used for most NASA test bars, was as follows: 1.5°C/min to 490°C with a 2 hr hold to complete binder removal, 3.4°C/min to 1175°C with a 12 hr hold, followed by 0.2°C/min to 1420°C with a 10 hr hold. Batches of up to 4 bars have been nitrided using this schedule with no evidence of damaging temperature gradients.

Table 6 includes nitrided composition and density data for all of the samples. Those which were submitted to NASA-Lewis for high temperature testing are indicated. Processing variations and nitriding schedules used for individual samples are also shown. Dimensions, shrinkages, and shape retention data are shown in Table 7.

Table 6. Bar Sample Phase Mixtures and Densities								
Sample	NASA test samples	Unique Processing	Firing Schedule*	% Nitrided wt gain	% Nitrided surface XRD	Surface α/β	Isopressed Si Density (%)	Nitrided Density (%)
9/22/92 #1			A	94.5	97.1...98.4	6.9...3.5	58.9	70.6
9/22/92 #2			A	94.4	95.2...98.5	5.9...4.1	58.9	69.5
10/15/92 #1			B	98.1	99.2...99.3	5.8...5.4		72.1
10/15/92 #2			B	97.9	97.5...100.0	7.2...3.9		71.5
11/16/92 #1		Vacuum burnout	C	87.0	94.3	3.0	58.7	68.9
11/16/92 #2		Vacuum burnout	C	87.0	92.8	2.8	58.6	68.7
12/19/92 #1	X		D	99.3	98.4...98.7	11.4...10.5	58.0	70.2
12/19/92 #2	X		D	99.4	99.0	10.5	59.7	71.2
12/20/92 #4			E	99.7	98.7	18.8	59.5	71.8
12/20/92 #5			E	99.6	98.7	15.8	59.3	72.1
12/20/92 #7	X	Air exposure	E	99.5	99.2...99.3	11.4...19.9	59.1	71.4
1/21/93 #1	X	Air exposure	E	99.5			60.0	71.5
1/21/93 #2	X		E	99.5	99.3	24.0	58.7	72.1
1/30/93 #2	X		E	99.5			58.8	71.7
1/29/93 #1			E	99.4	98.5	9.2	58.4	70.7
1/29/93 #2			E	98.9	99.1	10.2	58.0	70.0
2/7/93 #2	X		E	98.8	99.2	15.5	60.1	72.3
2/7/93 #3	X		E	99.1			59.1	71.5
2/7/93 #4			E	99.6	98.6-100	12.6	60.4	71.3
12/20/92 #6			E	99.5				71.2
1/29/93 #3a			E	99.0	99.0	19		71.1
1/29/93 #4a			E	99.4	100.0	6.7		70.2
1/30/93 #1			E	99.4			58.0	71.3

*Schedules are defined in a separate table.

Table 7. Bar Sample Dimensions and Shrinkages

Sample	Isopressed Dimensions			Nitrided Dimensions			Linear	Thick Daylight (% of t)		Width Daylight (% of w)	
	Length (mm)	Width (mm)	Thick (mm)	Length (mm)	Width (mm)	Thick (mm)	Shrinkage (%)	Concave side	Convex side	Concave side	Convex side
9/22/92 #1	48.70	6.05	2.35	48.49	6.05	2.38	0.4	13.9	21.4		
9/22/92 #2	48.70	6.25	2.66	48.41	6.08	2.81	0.6	7.2	29.8		
10/15/92 #1			5.83	45.33	6.05	6.11					
10/15/92 #2			6.00	48.48	6.17	5.92					
11/16/92 #1	48.69	6.13	4.86	48.40	6.14	4.95	0.6	12.3	12.8		
11/16/92 #2	48.78	6.14	4.94	48.64	6.16	5.02	0.3	14.4	13.2		
12/19/92 #1	48.92	6.22	4.00	48.37	6.15	4.12	1.1	10.4	18.7	5.8	2.9
12/19/92 #2	49.13	6.15	4.18	48.68	6.13	4.31	0.9	2.6	5.3	0.8	2.5
12/20/92 #4	49.06	6.12	4.02	48.51	6.10	4.11	1.1	1.5	9.6	3.3	4.2
12/20/92 #5	48.56	6.14	4.25	48.12	6.12	4.31	0.9	2.9	6.2	0.8	2.3
12/20/92 #7	49.00	6.18	4.17	48.51	6.18	4.25	1.0	7.2	11.1	3.7	4.5
1/21/93 #1	48.91	6.12	4.24	48.57	6.16	4.34	0.7	18.1	19.3	1.6	2.1
1/21/93 #2	48.66	6.12	4.43	48.31	6.10	4.43	0.7	2.9	5.2	2.5	4.6
1/30/93 #2	49.15	6.22	4.14	48.59	6.18	4.22	1.1	3.6	3.6	2.3	2.9
1/29/93 #1	48.50	6.11	4.35	48.28	6.10	4.40	0.4	13.3	16.2	6.7	7.1
1/29/93 #2	49.00	6.19	4.30	48.62	6.19	4.37	0.8	8.1	13.4	3.7	7.4
2/7/93 #2	48.79	6.09	4.31	48.38	6.09	4.40	0.8	4.6	10.7	2.3	4.0
2/7/93 #3	48.80	6.10	4.40	48.33	6.09	4.49	1.0	4.5	6.8	0.0	1.7
2/7/93 #4	48.65	6.03	4.37	48.27	6.08	4.51	0.8	6.2	13.5	2.1	1.7
12/20/92 #6	48.80	6.12	4.24	48.45	6.10	4.34	0.7				
1/29/93 #3a				29.74	6.20	3.87					
1/29/93 #4a				31.96	6.21	4.16					
1/30/93 #1	49.40	6.12		49.13	6.15	4.20	0.6				

Table 8. Bar Sample Nitriding Schedules

A	B	C	D	E
1.8°C/min to 490°C No hold	1.8°C/min to 490°C No hold	1.8°C/min to 490°C No hold	1.5°C/min to 490°C 2 h hold	1.5°C/min to 490°C 2 h hold
3.4°C/min to1245°C 4.5 h hold	3.4°C/min to1200°C 4.5 h hold	3.4°C/min to1200°C 4.5h hold	3.4°C/min to1200°C 8 h hold	3.4°C/min to1175°C 12 h hold
0.5°C/min to 1400°C 10 h hold	0.5°C/min to 1400°C 10 h hold	0.5°C/min to 1410°C 10 h hold	0.5°C/min to 1400°C 10 h hold	0.2°C/min to 1420°C 10 h hold

The percentage of Si which has been converted to nitride was determined by two methods. Bulk values are based on weight gain during nitriding, assuming complete loss of binder. Surface conversions and α/β ratios were determined from XRD profiles. Where two values are shown for XRD data, these are results for two different surfaces of the sample. Most of the optimum nitriding schedule sample weight gains indicate >99.5% conversion, and XRD data agrees well. α/β ratios increased with decreasing initial nitriding temperature. A dependence on processing exposures other than temperature is also indicated from a comparison of this data with as-synthesized Si data. One expects an α/β ratio < 5 for as-synthesized Si powers nitrided at or above 1100°C.[14] Surface α/β ratios of nitriding schedule E samples range between 9 and 20.

Isopressed and nitrided densities were calculated from sample weights and measured dimensions. Widths and thicknesses shown in Table 7 are averages of 4 - 5 measurements. Unfired Si densities were 58-60% of theoretical, ~1-2% lower than typically achieved with colloidally pressed samples. Further optimization of the spray drying process should improve these values. Nitrided densities agree well with those projected from the green densities, assuming no bulk dimensional changes occur during nitriding. Low shrinkages (green isopressed → nitrided) of the bar lengths (0.3 - 1.1%) support this assumption.

While these shrinkage values are low, they are not representative of the near net shape capability of this reaction bonding process. Shrinkages for colloidally pressed parts which have near theoretical green densities have been as low as 0.1%. Shrinkages (length basis) between isopressed and nitrided states are plotted in Figure 29 as a function of isopressed density. Normally, higher green densities should yield lower shrinkages. The random distribution of values shown in Figure 29 suggests that the data is subject to a random measurement error that is larger than the shrinkage values.

The thickness daylight and width daylight are rough estimates of the amount of warping in the respective directions. Measurements were made on the as-nitrided parts. "Daylight" is defined as follows:

Concave side thickness daylight = A/(ave thickness)*100
Convex side thickness daylight = B/(ave thickness)*100

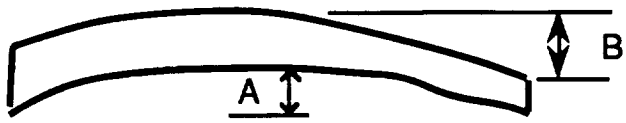

The calculated daylights in Table 7 indicate that all samples were bowed. Bowing was greater in the thickness, or die pressing, direction. Many samples were also tapered and many had a difference in daylight between the concave and convex sides of the sample.

III. Discussion

The primary reason for spray drying the Si powder was to uniformly incorporate a binder while increasing the powder size so that it would be free flowing. An additional benefit was the increased protection of the powder against oxidation during processing.

In this and a related program, samples were exposed to air at one of several processing stages to determine the effect on nitriding. The purpose was to determine whether the spray dried powder surfaces were protected from oxidation, and if so, when in processing this protection was lost. For example, samples 12/20/92 #7 and 1/21/93 #1 were air exposed after isopressing, while being loaded into the nitriding furnace. Other samples were made from spray dried powder which had been stored in air for several months, or were die pressed in air. The percent conversion and α/β ratios agree with those of other samples after the same nitriding schedule. None of these samples showed the low conversions and slow reaction rates observed for as-synthesized powder which has been oxidized. Further work is necessary to define the relationship of binder content with degree of protection, but it appears that indefinite room temperature air exposure prior to binder removal has no effect on the nitriding behavior of the spray dried powder.

Two binder related problems were encountered during transition from the 1.2 cm diameter (1/2 inch) TGA samples to the larger bar samples. The combination of the furnace configuration and low gas flow rates caused uncontrolled binder re-distribution within the furnace as the cooler, closed end of the furnace tube reached maximum burnout temperature. In the worst case, X-ray diffraction analyses showed binder redeposited on the sample surface and reacted to form SiC.

Minimum schedules which completely removed the binder from the hot zone of the furnace had to be defined. Two schedule C nitriding runs were made in which the binder removal portion was carried out in vacuum. In the first run, samples were heated at 1.8°C/min to 490°C and then immediately heated in N_2

at ~ twice the initial rate to nitriding temperatures. The second run differed only in the addition of a 2 hr hold at 490°C. Binder removal was monitored with a thermistor pressure gauge located between the furnace and vacuum pump. As shown in Figure 30, the pressure vs. time curves of the two runs are nearly identical until the temperature schedules vary. The furnace pressure increased significantly as the temperature approached 300°C, indicating binder volatilization. The pressure peaked and was decreasing as the temperature reached 490°C; however it returned to initial levels, indicating complete burnout, only after the hold at 490°C.

The second binder related problem was cracking of bar samples when heated according to binder removal schedules which were found to be adequate for the thinner TGA samples. The optimum burnout rate provides minimal exposure of the Si powder to moderate temperature levels where it is unprotected from oxidation. Decreasing the initial heating rate from 1.8 to 1.5°/min eliminated the cracking problem while adding only 20% to the burnout time.

IV. CONCLUSIONS

These results showed that test bars can be made from the small diameter Si powders using rather conventional procedures. The nature of the powders and the nitriding reaction require attention to the details of some processing steps. Volatilized binders must be completely removed from the furnace to avoid subsequent reactions with the powders with continued heating to nitriding temperature levels. As with conventional ceramic processes, excessive binder removal rates cause cracks which are not healed during subsequent consolidation steps. Using Si powders dispersed in xylene and polystyrene, spray dried powders nitrided rapidly to completion even with long exposures to air. Excessive warping remained the only unresolved problem in forming flexural test samples that could be measured without machining.

The warping occurred during warm isopressing, indicating that density gradients existed in the straight, die pressed bars. These gradients are probably related to non-uniform filling and/or non-uniformities in size or density of the spray dried powder particles. The spray dried particles formed with this solvent-binder combination had appropriate dimensions (~ 10 μm diameter), but they did not flow well because they were tacky. Optimization of the spray drying process was beyond the scope of this program, but can be considered in future work.

REFERENCES

1. Lightfoot, A., R.S. Parikh, J.S. Haggerty, and B.W. Sheldon, *Nitridation of Binder and Solvent Exposed High Purity Silicon Powder*, submitted to J. AM. CERAM. SOC.

2. Sheldon, B.W. and J.S. Haggerty, *The Nitridation of High Purity, Laser-Synthesized Silicon Powder to Form Reaction Bonded Silicon Nitride*, CERAM. ENG. SCI. PROC. **9** [7-8] 1061-71 (1988).

3. Sheldon, B.W., and J.S. Haggerty, *The Formation of Reaction Bonded Si_3N_4 at Low Temperatures and in Short Times*, CERAM. ENG. SCI. PROC. **10** [7-8] 784-793 (1989).

4. Sheldon, B.W., and J.S. Haggerty, *Nitrogen Adsorption onto Silane Derived Silicon Powders*, J. AM. CERAM. SOC. **74** [6] 1417-24 (1991).

5. Sheldon, B.W., J. Szekely, and J.S. Haggerty, *Formation of Reaction Bonded Silicon Nitride from Silane Derived Silicon Powders: Macroscopic Kinetics and Related Transport Phenomena*, J. AM. CERAM. SOC. **75** [3] 677-85 (1992).

6. QPAC™ product literature, Air Products and Chemicals, Inc., Emmaus, PA 18049.

7. Bhatt, R.T., *Effects of Fabrication Conditions on the Properties of SiC Fiber Reinforced Reaction-Bonded Silicon Nitride Matrix Composites (SiC/RBSN)*, NASA Technical Memorandum 88814, January 1986.

8. Seyferth, D., and G.H. Wiseman, *High-Yield Synthesis of Si_3N_4/SiC Ceramic Materials by Pyrolysis of a Novel Polyorganosilazane*, J. AM. CERAM. SOC., **67** [7], C-132-3 (1984).

9. Han, H.N., D.A. Lindquist, J.S. Haggerty, and D. Seyferth, *Effect of Silicon Exposure on Pyrolysis of Preceramic Polysilazane*, Materials Research Society 1991 Fall Meeting, Boston, MA, December 1991, MAT. RES. SOC. SYMP. PROC. **249**, 391-396 (1992).

10. Pouchert, C.J., The Aldrich Library of Infrared Spectra, Aldrich Chemical Co., Milwaukee. 3rd edition (1981) p. 566H (Xylenes). 2nd edition (1975) pages 499B (Toluene), 1349G (Polymethyl methacrylate) and 1355B (Polystyrene).

11. Nakamoto, K., Infrared and Raman Spectra of Inorganic and Coordination Compounds, 4th edition, John Wiley & Sons, 1986.

12. Socrates, G., Infrared Characteristic Group Frequencies, Chichester, NY, John Wiley & Sons, 1980.

13. Kramer, T.M., Surface Chemistry of Hydrogenated Silicon and Silicon Carbide Powders, Sc.D. Thesis, Department of Materials Science and Engineering, Massachusetts Institute of Technology, May, 1988.

14. Sheldon, B. W., The Formation of Reaction Bonded Silicon Nitride From Silane Derived Silicon Powders, Sc.D. Thesis, Department of Materials Science and Engineering, Massachusetts Institute of Technology, Cambridge, MA, January 1989.

15. Parikh, R.S., A. Lightfoot, J.S. Haggerty, and B.W. Sheldon, *The Effects of Trace O_2 Levels on the Nitriding Kinetics of High Purity Si Powders to Form Reaction Bonded Silicon Nitride*, to be submitted to J. AM. CERAM. SOC.

16. Lightfoot, A., J. Sigalovsky, and J.S. Haggerty, *Relationships between Toughness and Microstructure of Reaction Bonded Si_3N_4*, CERAM. ENG. SCI. PROC. **13** [9-10] 1024-1031 (1992).

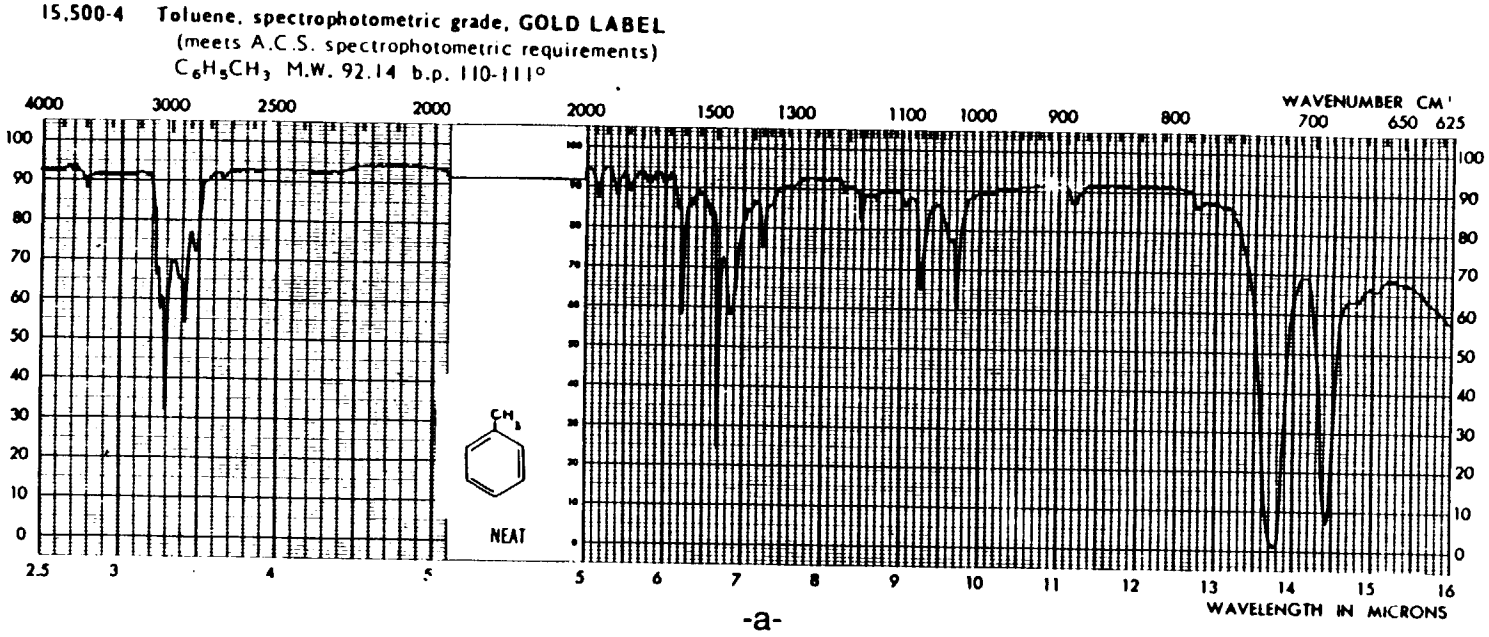

-a-

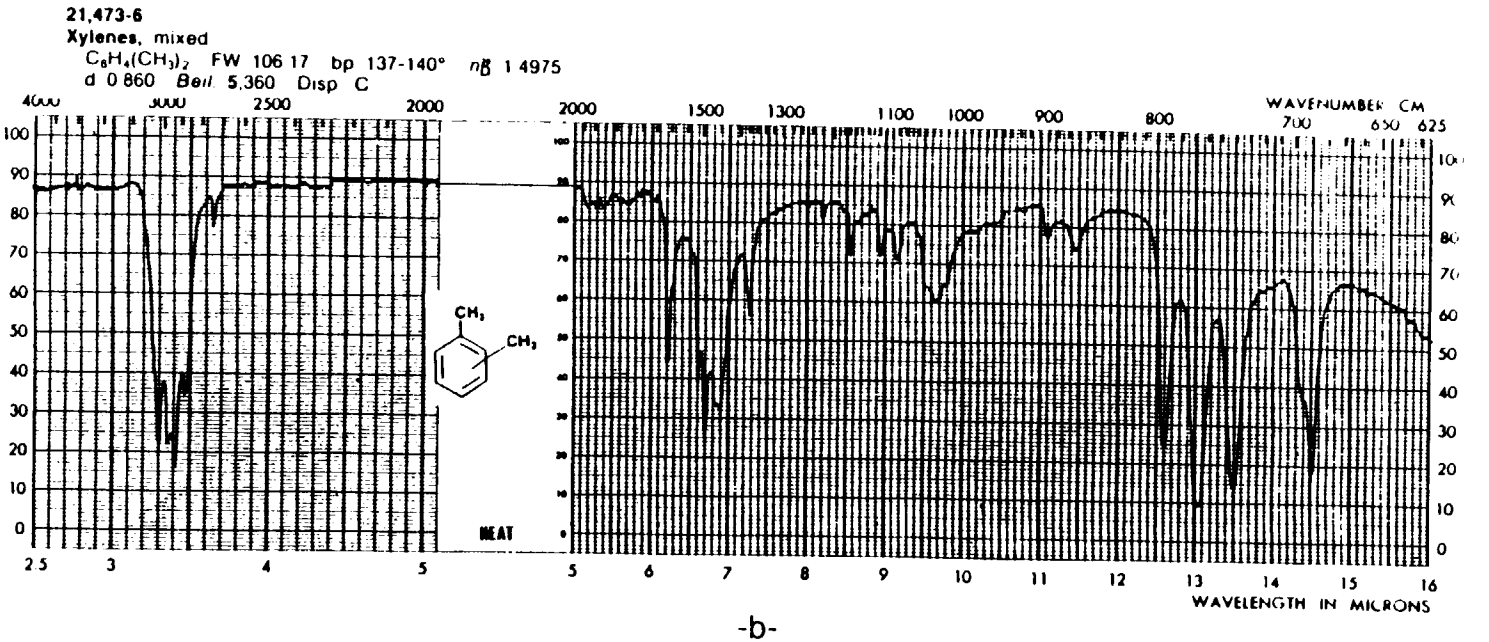

-b-

Figure 1a-b. Spectra for (a) toluene and (b) xylene.

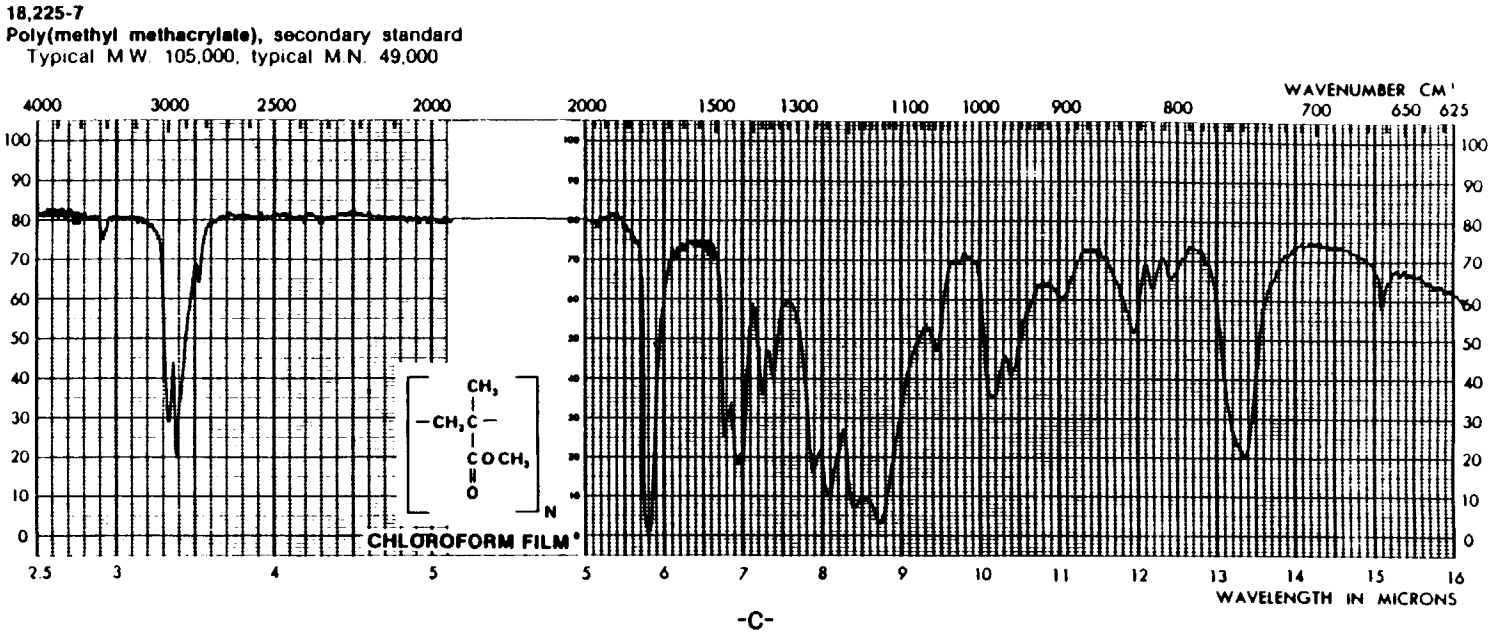

-c-

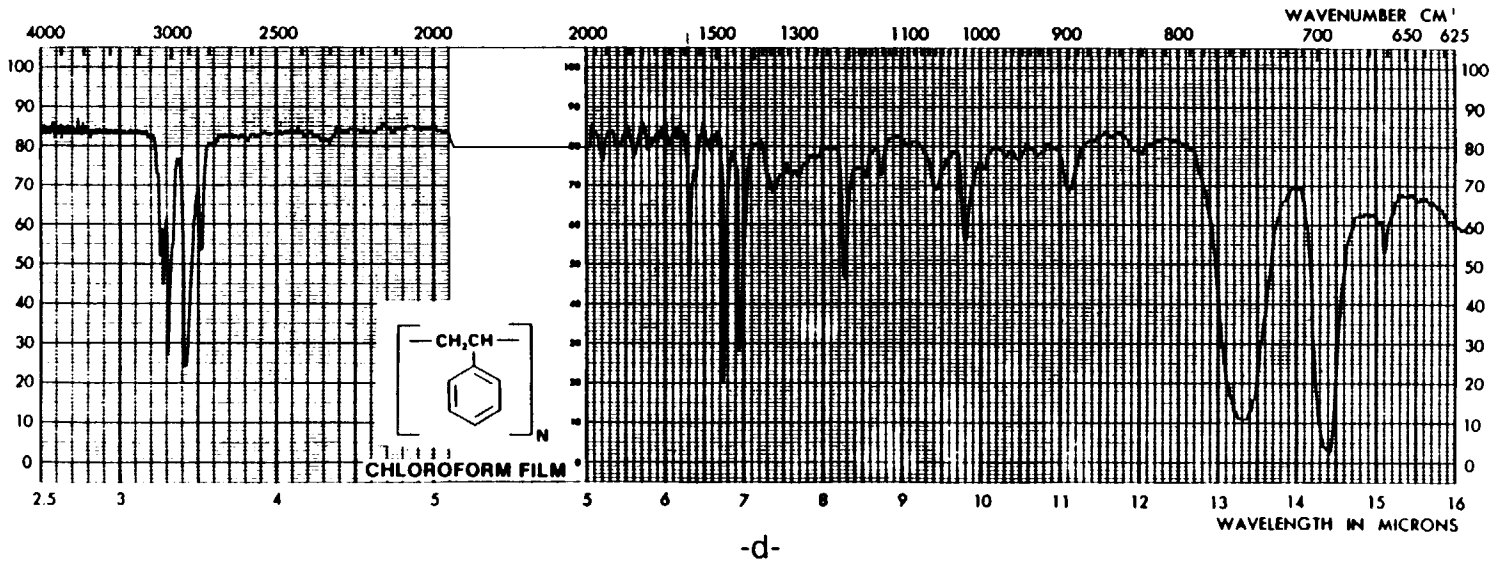

-d-

Figure 1c-d. Spectra for (c) polymethylmethacrylate and (d) polystyrene.

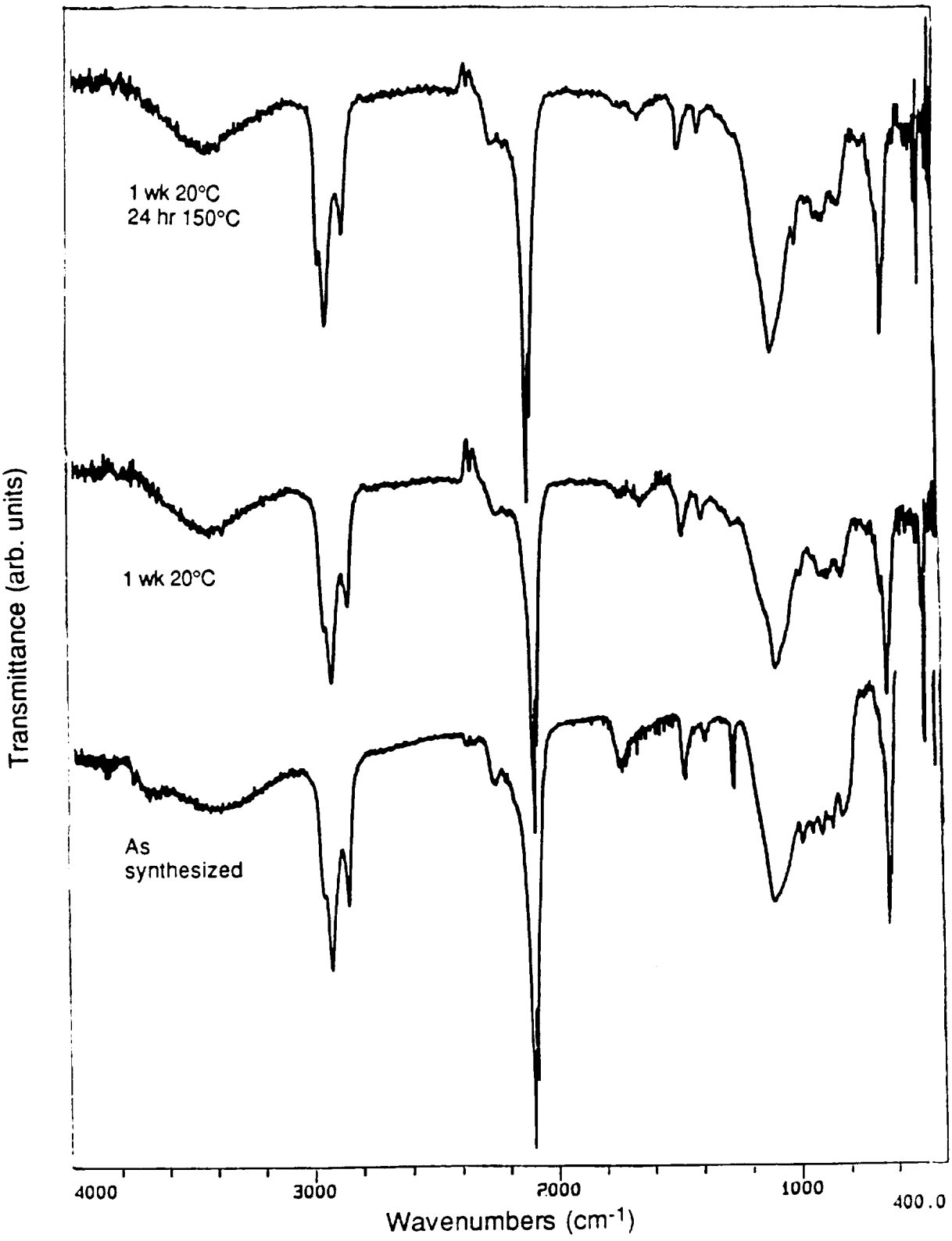

Figure 2. DRIFT spectra of Si powders exposed to N_2 for indicated times and temperatures.

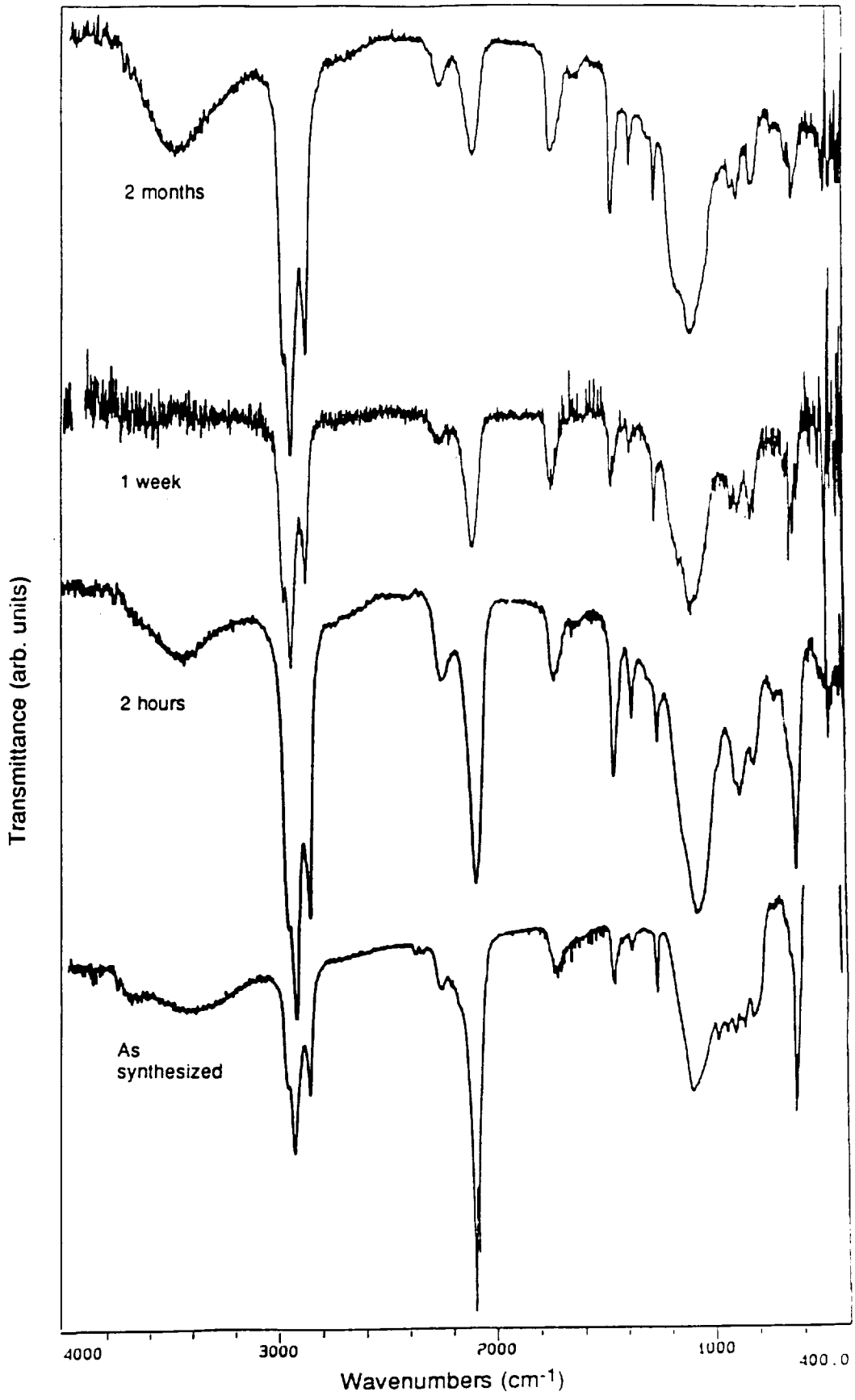

Figure 3. DRIFT spectra of Si powders after toluene exposures for indicated times at 20°C followed by N_2 for 24h at 20°C.

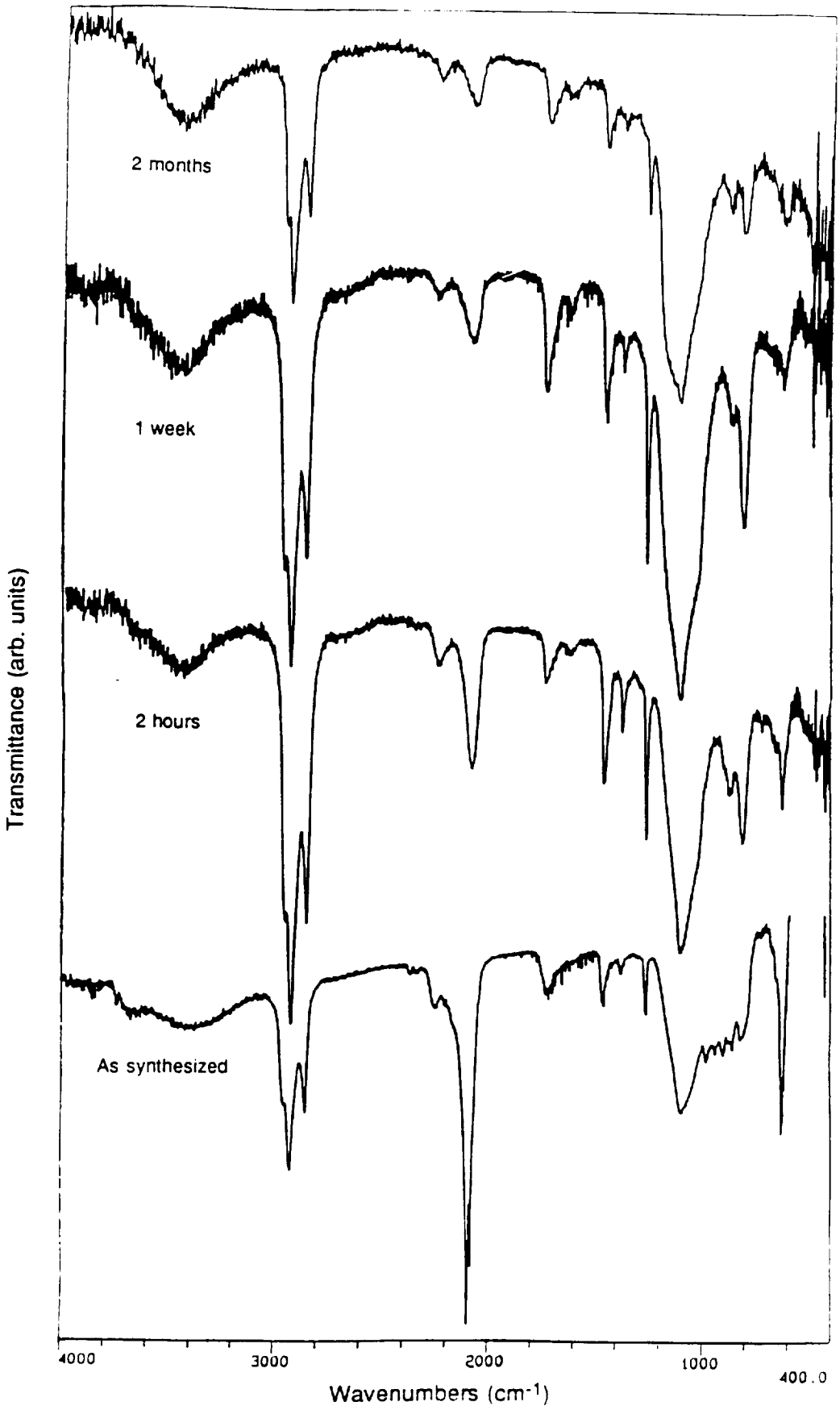

Figure 4. DRIFT spectra of Si powders after toluene exposure for indicated times at 20°C followed by N_2 for 24h at 150°C.

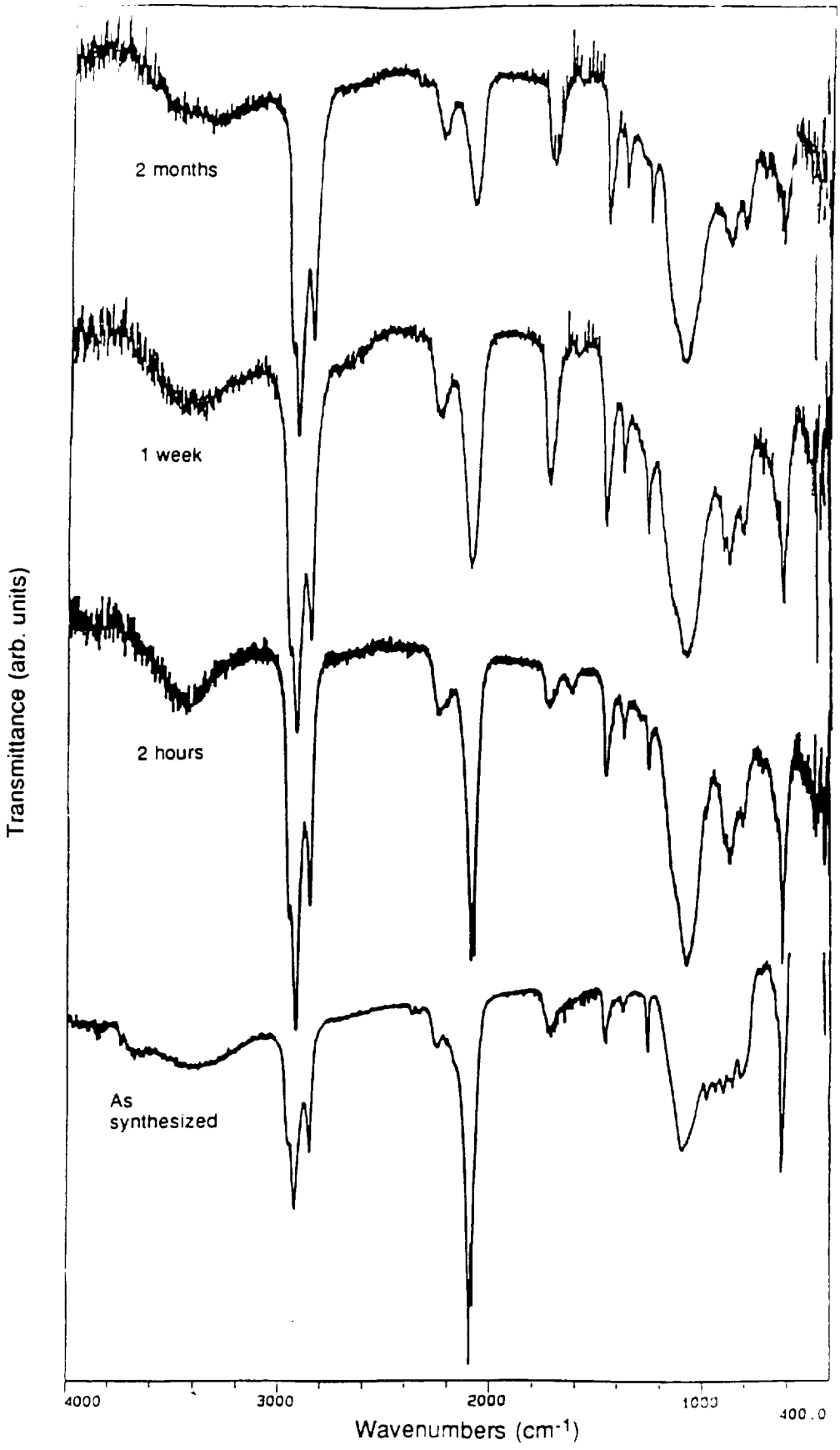

Figure 5. DRIFT spectra of Si powders after xylene exposure for indicated times followed by N_2 for 24h at 20°C.

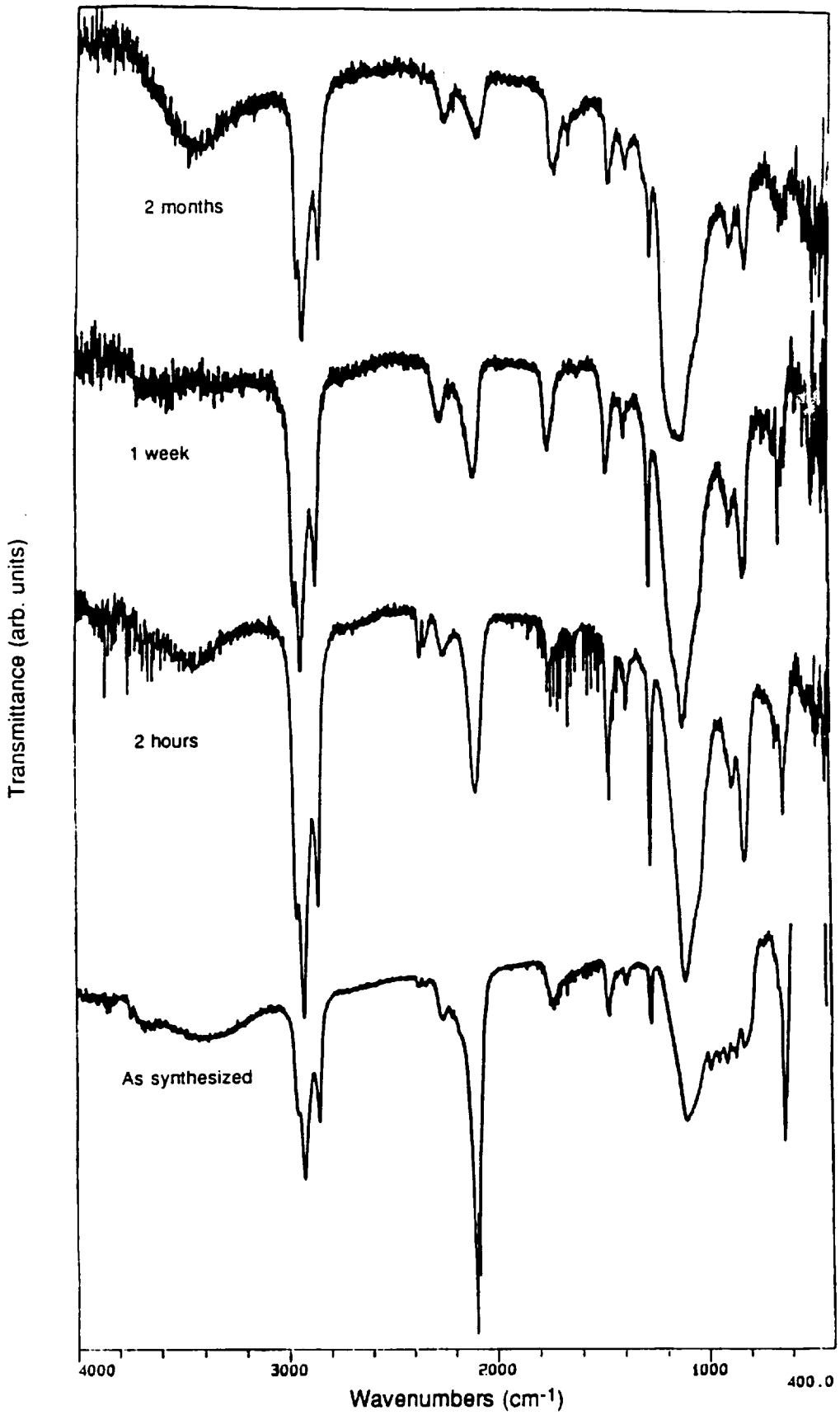

Figure 6. DRIFT spectra of Si powders after xylene exposure for indicated times followed by N_2 for 24h at 150°C.

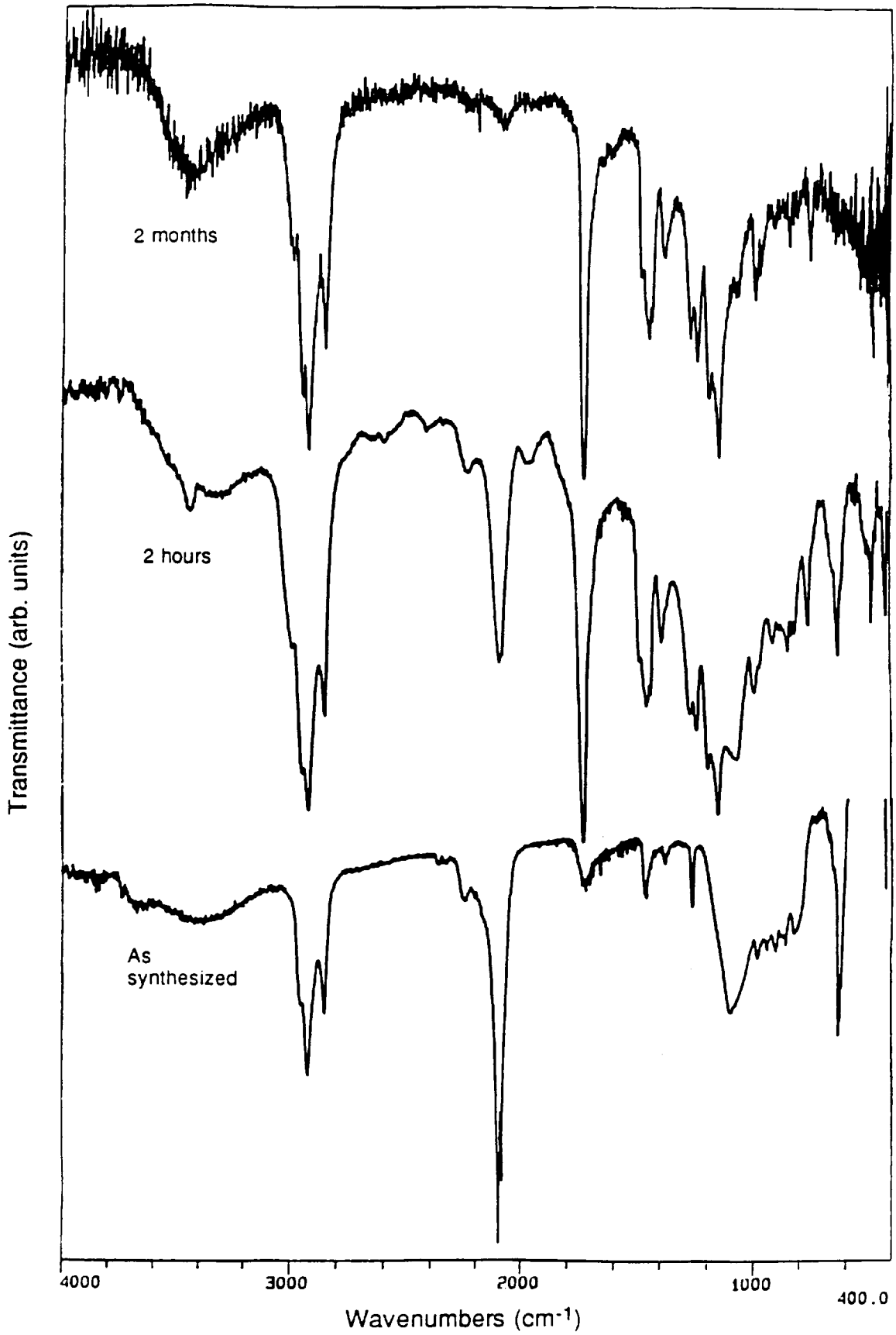

Figure 7. DRIFT spectra of Si powders after xylene plus PMMA exposure for indicated times followed by N_2 for 24h at 20°C.

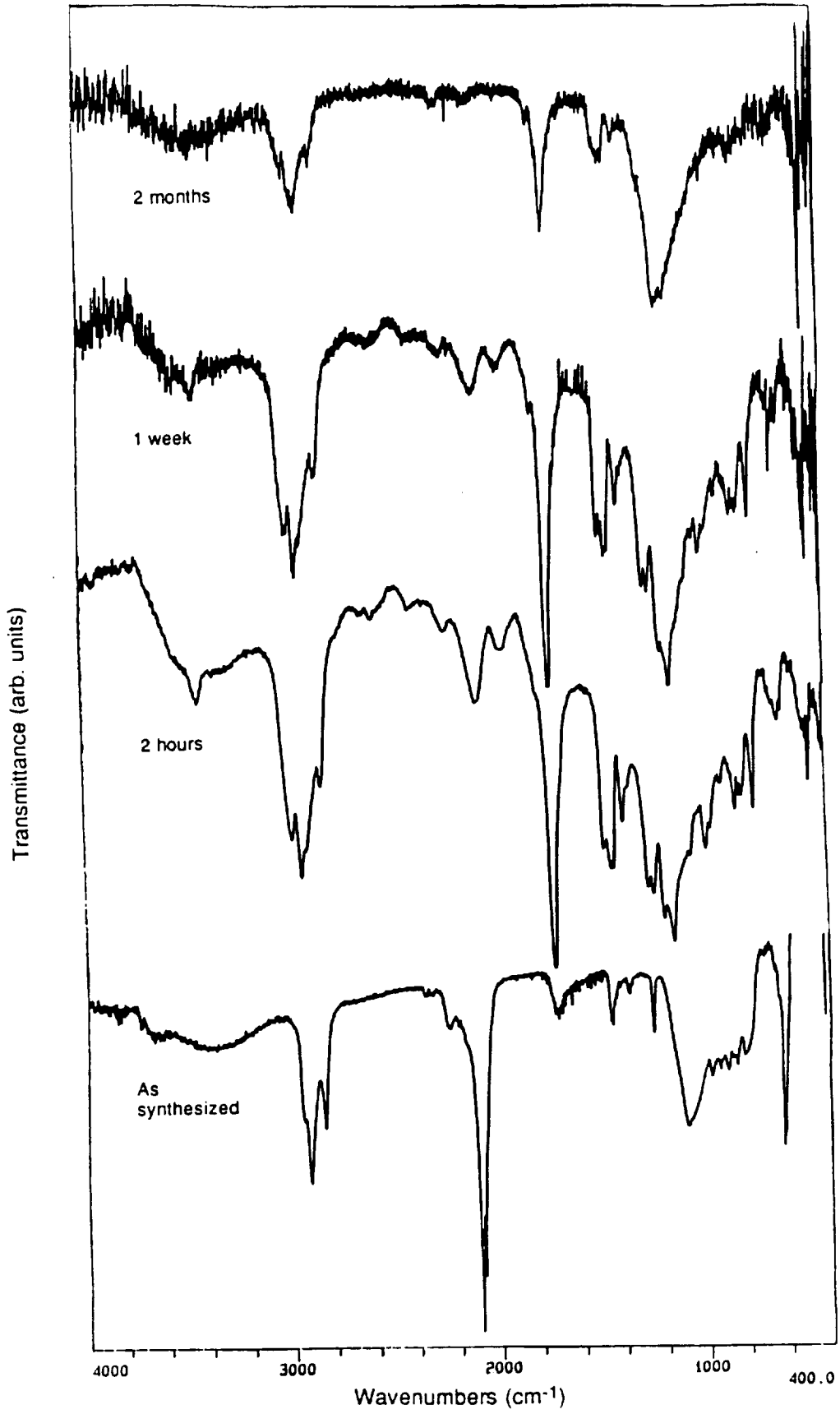

Figure 8. DRIFT spectra of Si powders after xylene plus PMMA exposure for indicated times followed by N_2 for 24h at 150°C.

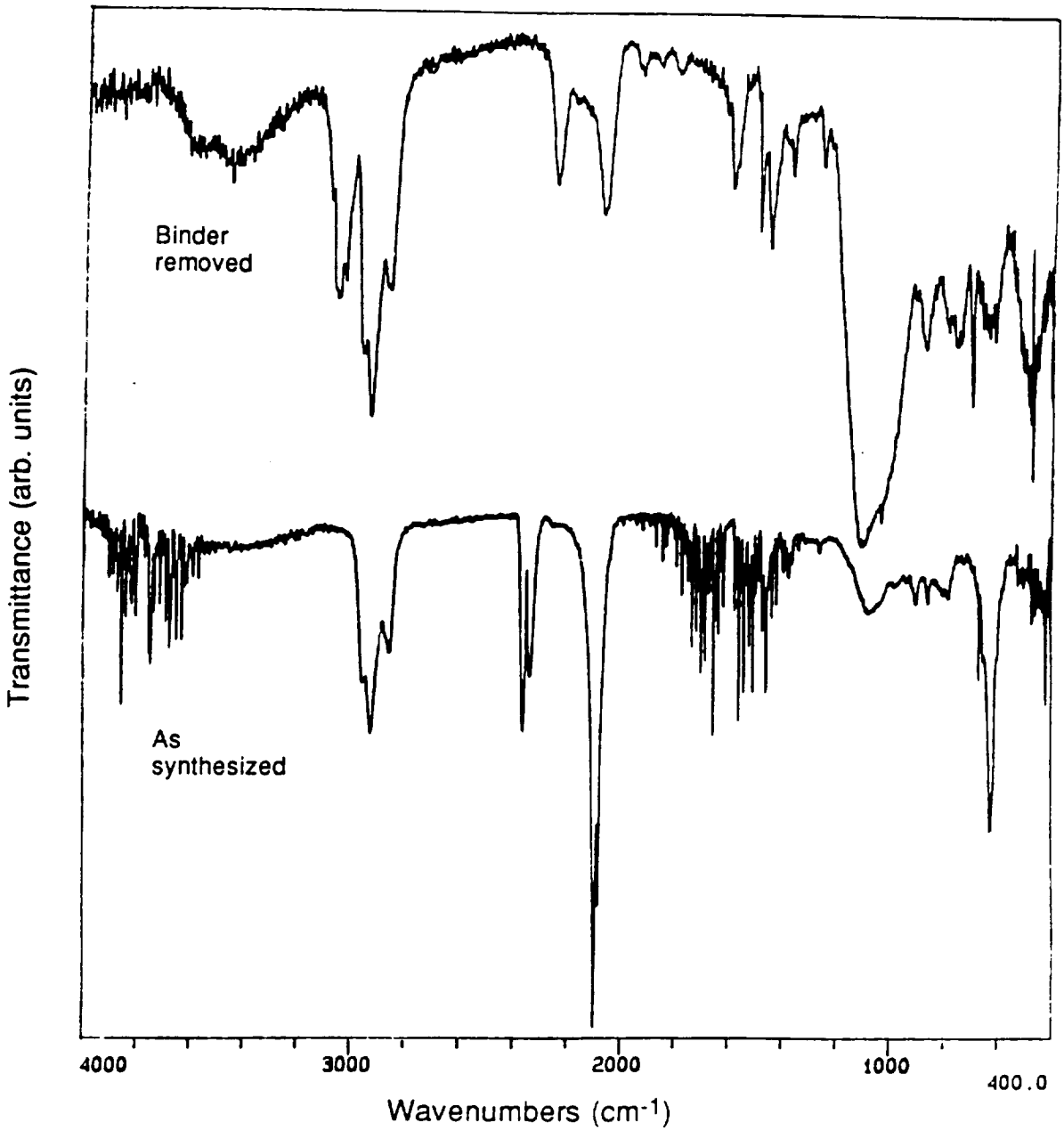

Figure 9. DRIFT spectra of spray dried Si powders after xylene and polystyrene exposure followed by binder burnout in N_2 at 480°C.

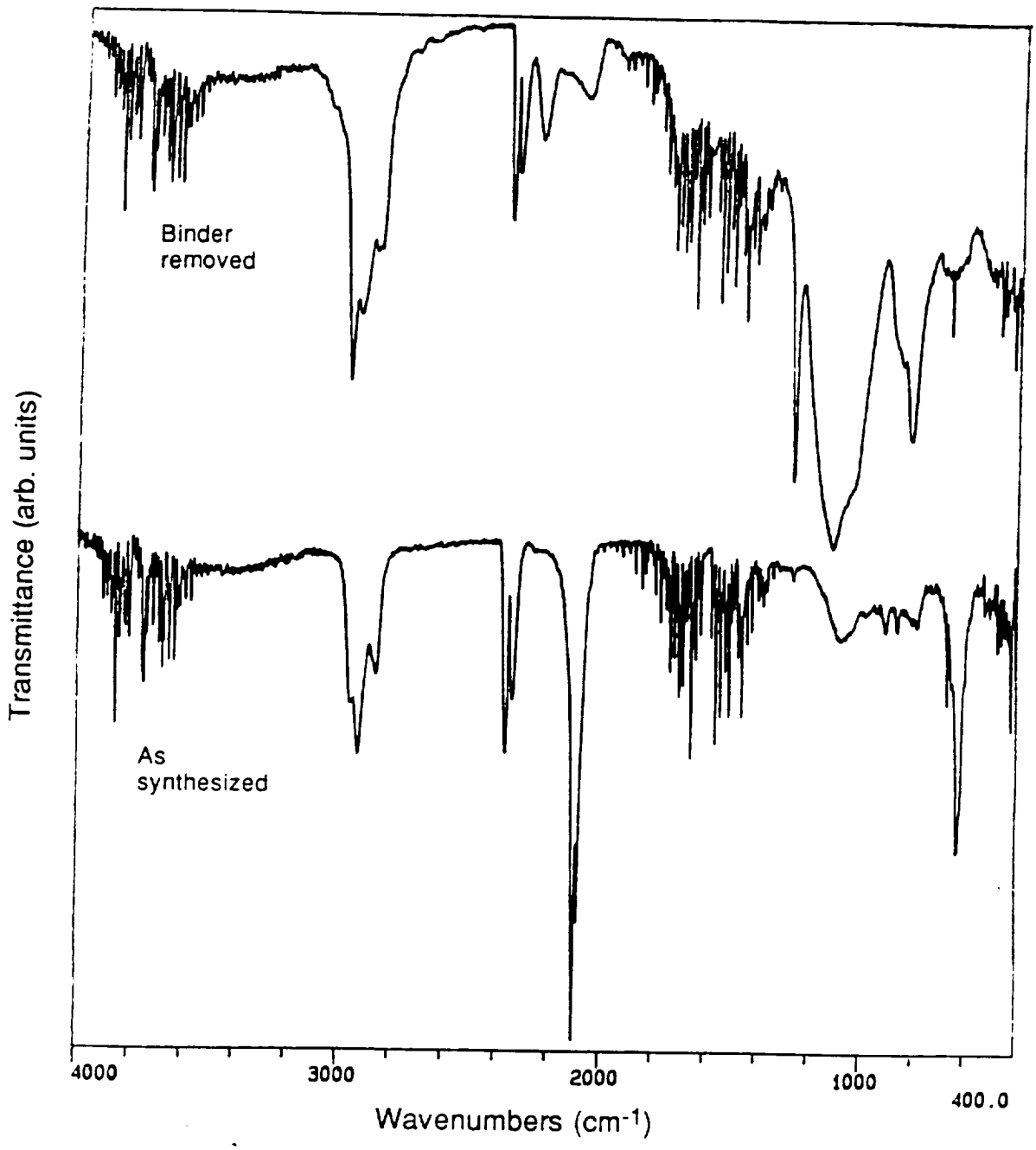

Figure 10. DRIFT spectra of spray dried Si powders after toluene and PMMA exposure followed by binder burnout in N_2 at 450°C.

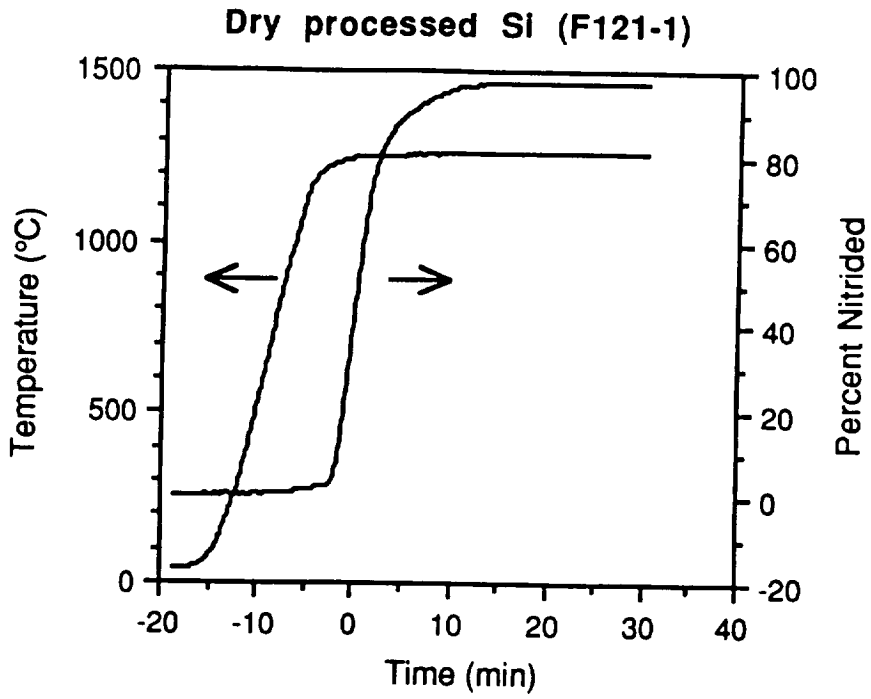

Figure 11. TGA results for dry processed Si powder subjected to indicated heating schedule in UHP N_2. (Sample F121-1)

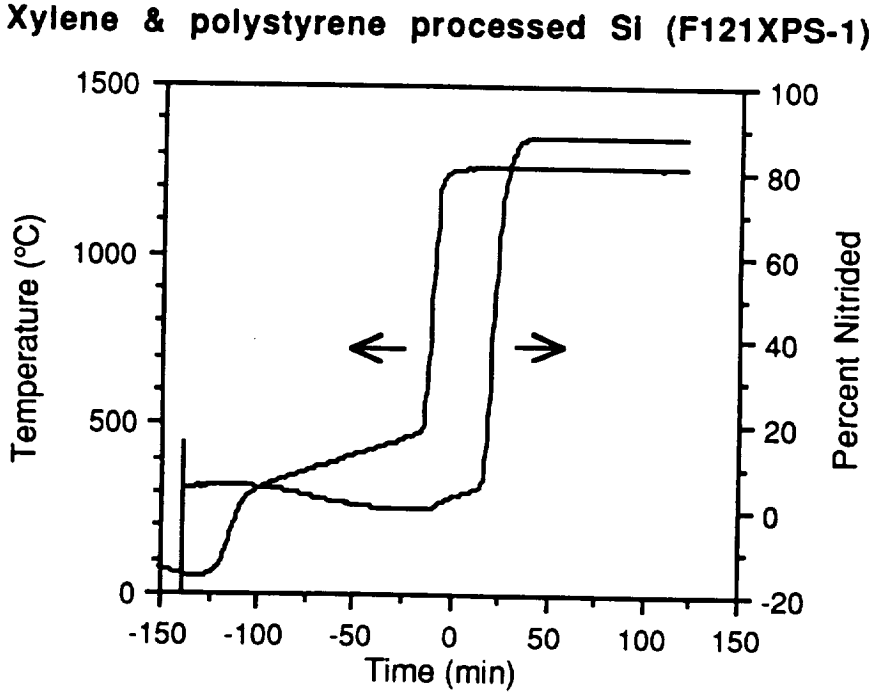

Figure 12. TGA results for xylene and polystyrene processed Si powder subjected to indicated heating schedule in UHP N_2. (Sample F121XPS-1)

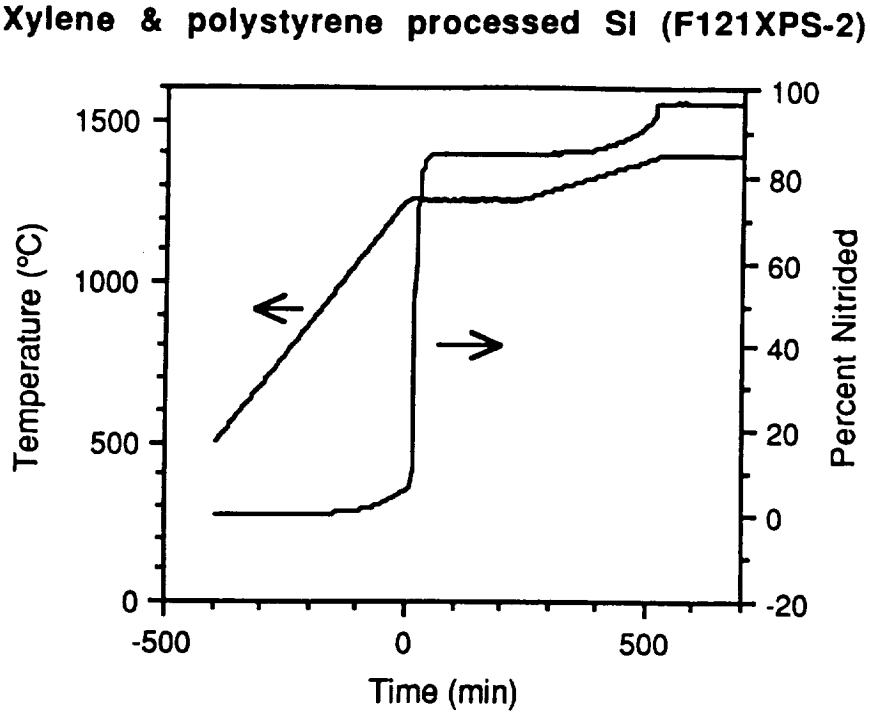

Figure 13. TGA results for xylene and polystyrene processed Si powder subjected to indicated heating schedule in UHP N_2. (Sample F121XPS-2)

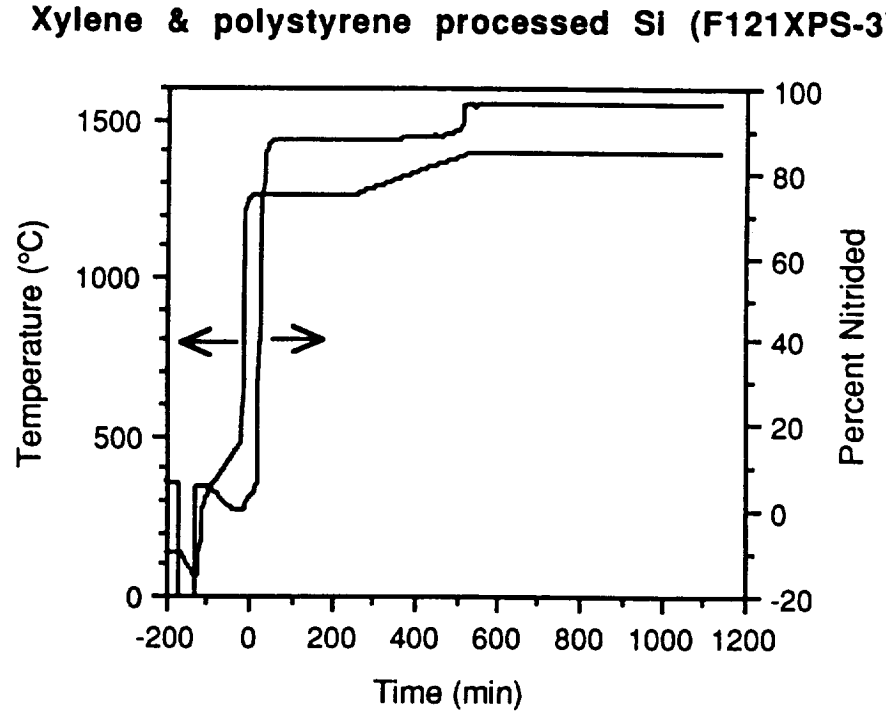

Figure 14. TGA results for xylene and polystyrene processed Si powder subjected to indicated heating schedule in UHP N_2. (Sample F121XPS-3)

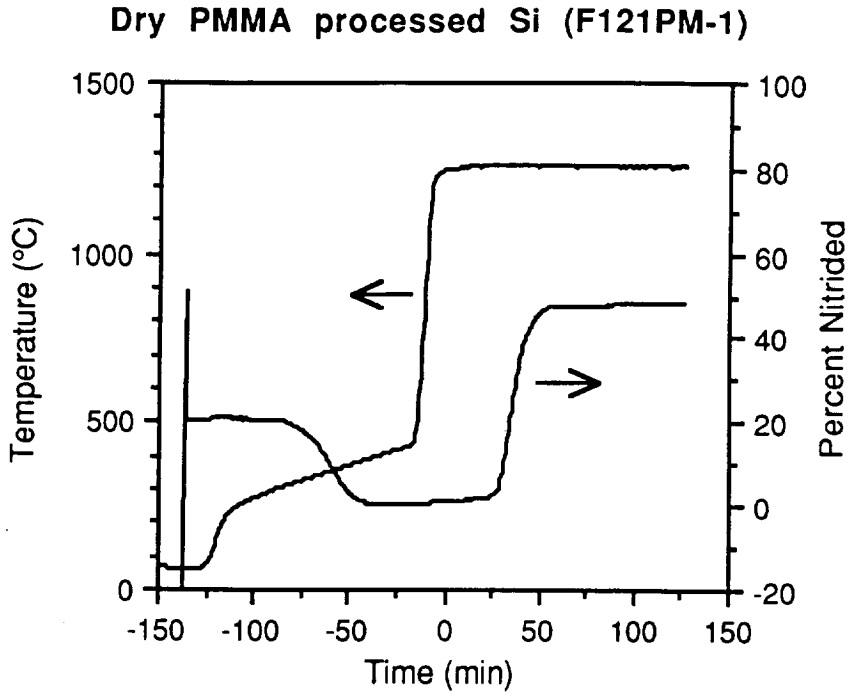

Figure 15. TGA results for PMMA processed Si powder subjected to indicated heating schedule in UHP N_2. (Sample F121PM-1)

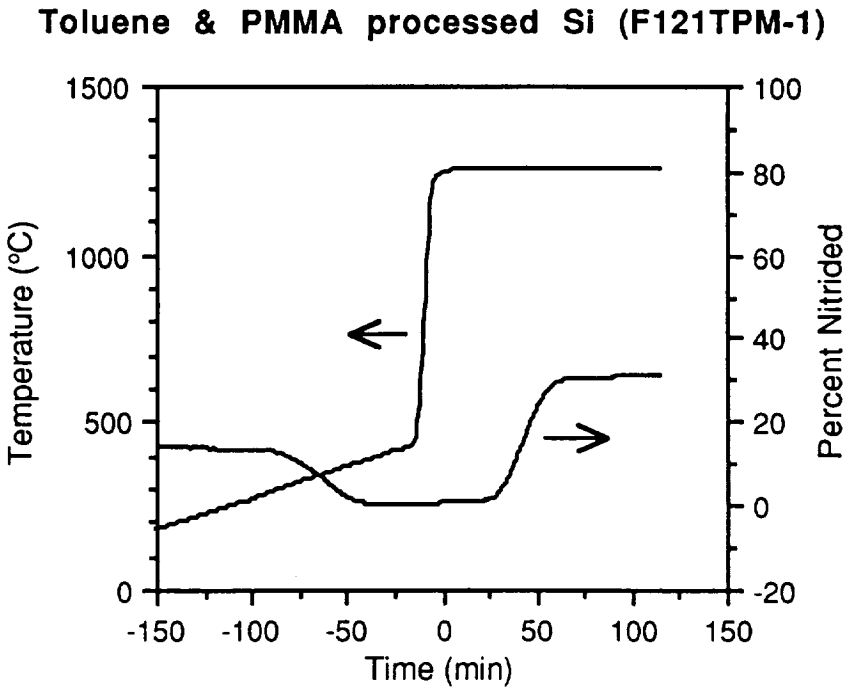

Figure 16. TGA results for toluene and PMMA processed Si powder subjected to indicated heating schedule in UHP N_2. (Sample F121TPM-1)

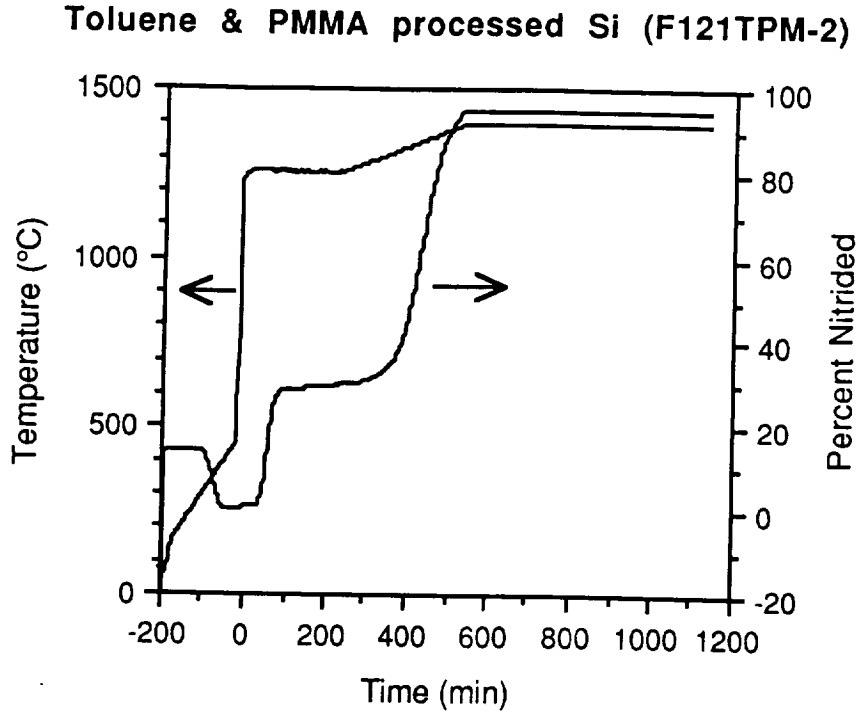

Figure 17. TGA results for toluene and PMMA processed Si powder subjected to indicated heating schedule in UHP N_2. (Sample F121TPM-2)

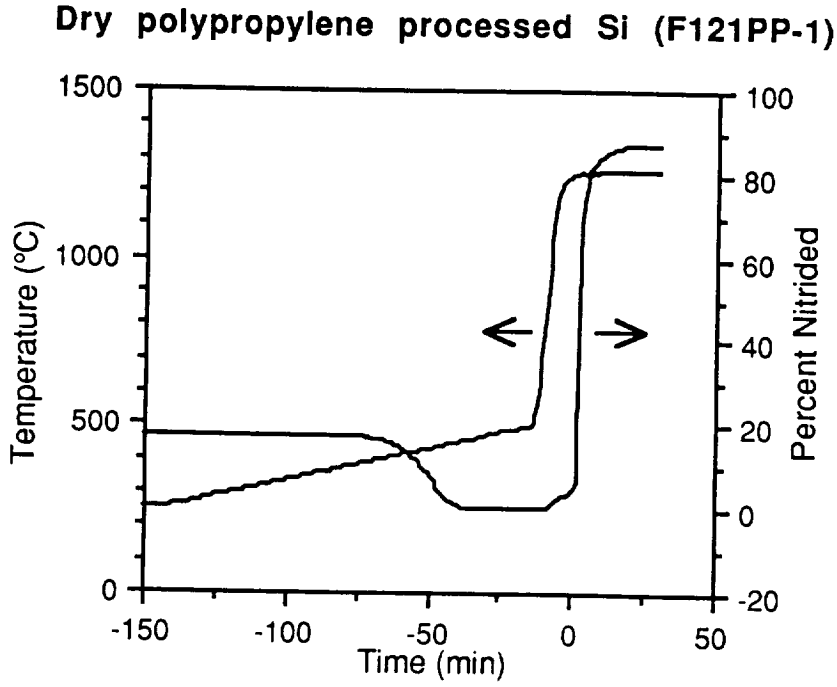

Figure 18. TGA results for polypropylene processed Si powder subjected to indicated heating schedule in UHP N_2. (Sample F121PP-1)

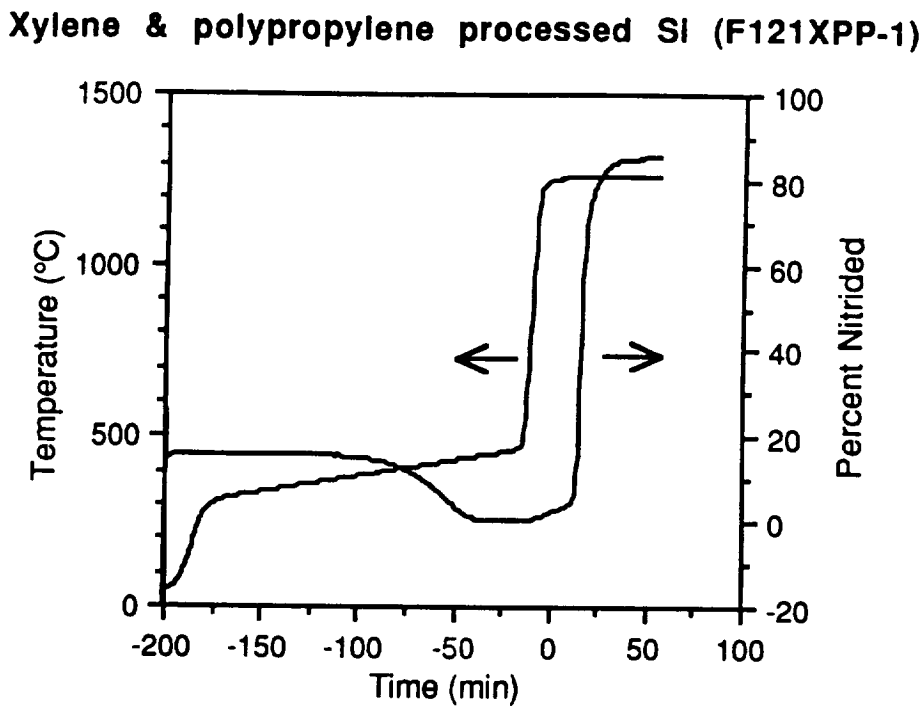

Figure 19. TGA results for xylene and polypropylene processed Si powder subjected to indicated heating schedule in UHP N_2. (Sample F121XPP-1)

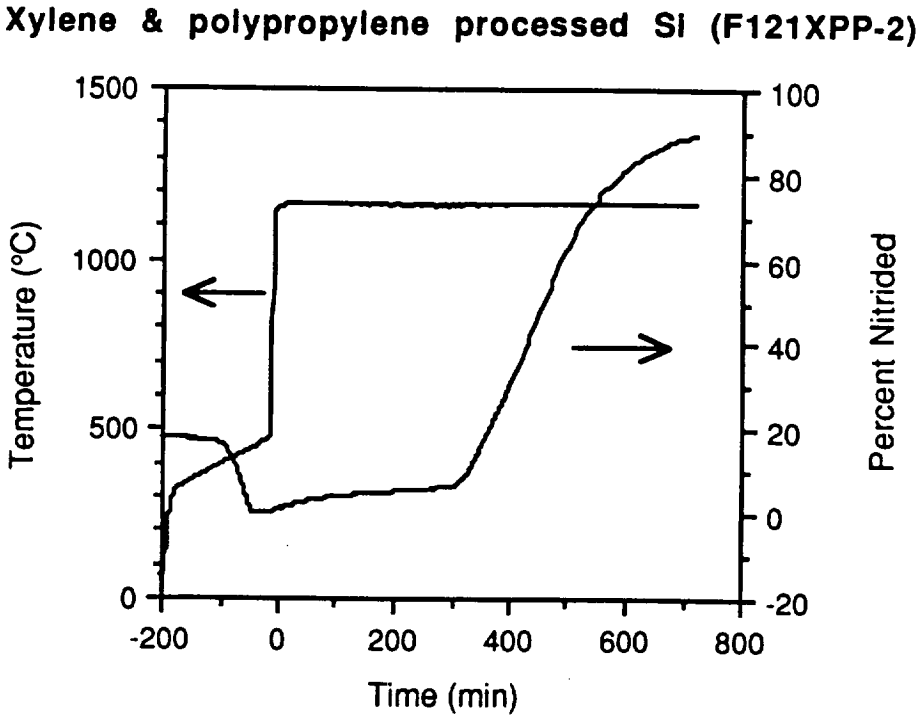

Figure 20. TGA results for xylene and polypropylene processed Si powder subjected to indicated heating schedule in UHP N_2. (Sample F121XPP-2)

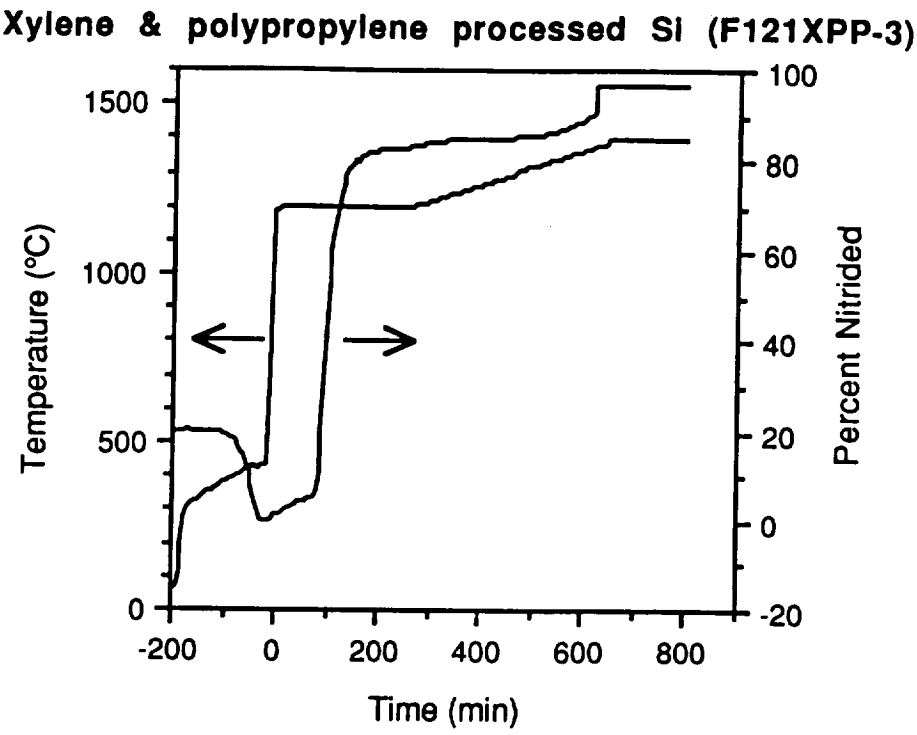

Figure 21. TGA results for xylene and polypropylene processed Si powder subjected to indicated heating schedule in UHP N_2. (Sample F121XPP-3)

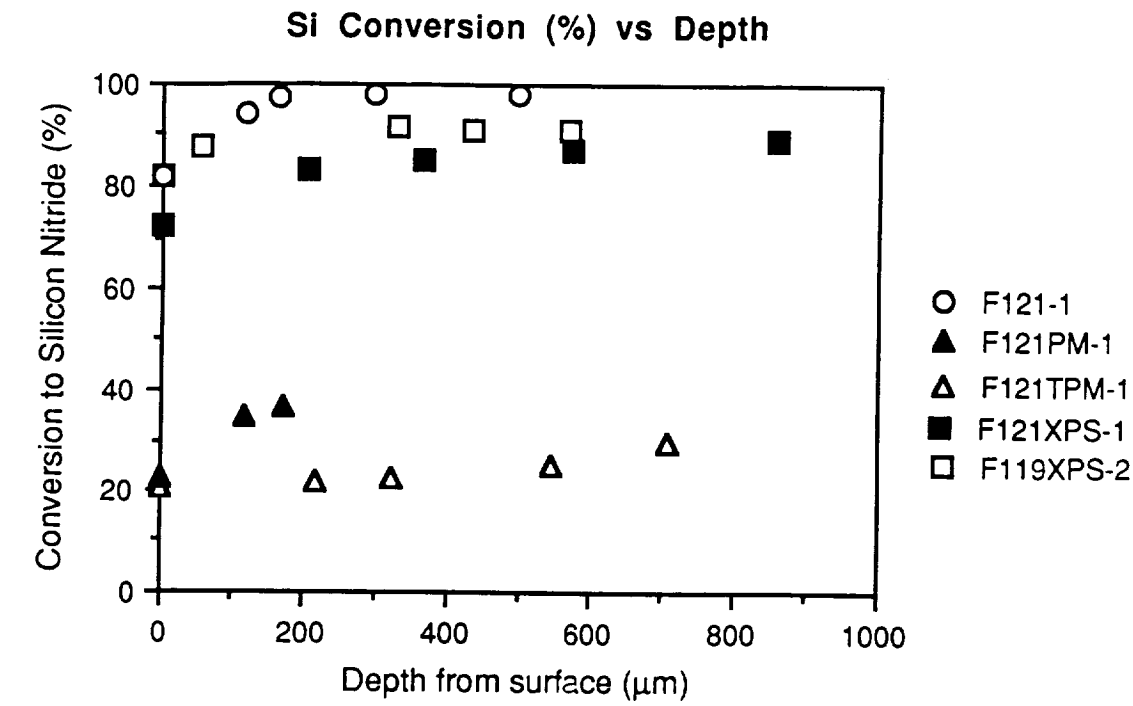

Figure 22. Extent of conversion defined by quantitative X-ray diffraction as a function of distance from exterior as-nitrided surface for a dry Si sample and four polymer and solvent exposed samples. Processing histories are summarized in Table 3.

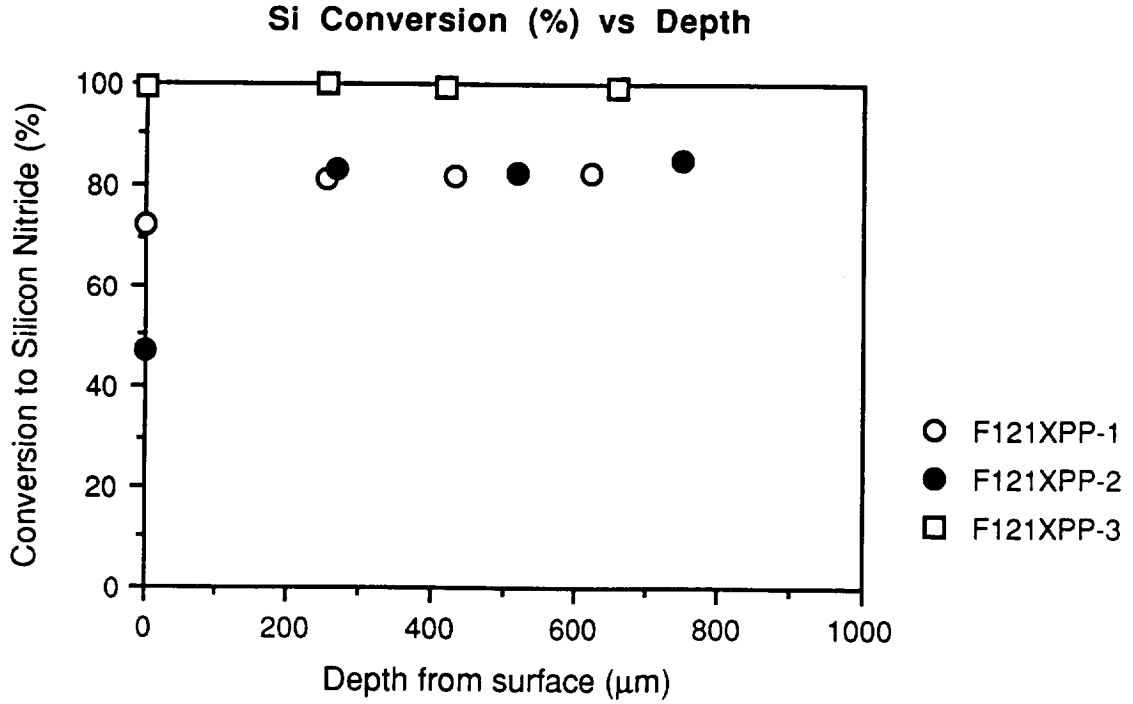

Figure 23. Extent of conversion defined by quantitative X-ray diffraction as a function of distance from exterior as-nitrided surface for three polypropylene and xylene exposed samples. Processing histories are summarized in Table 3.

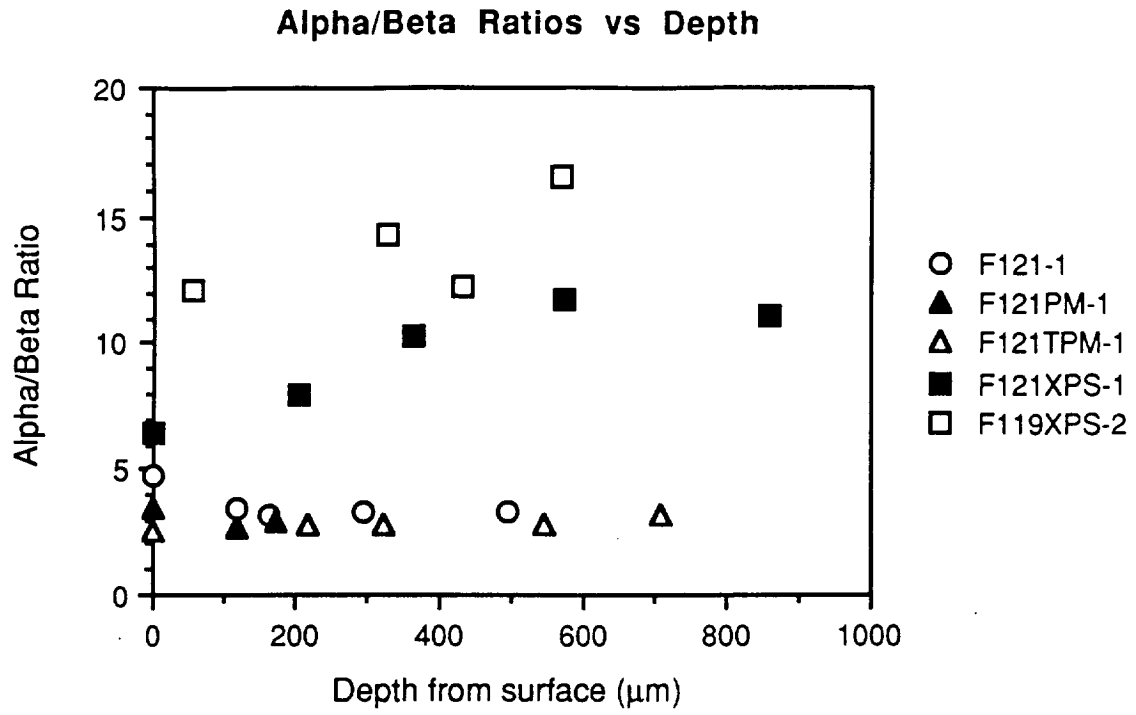

Figure 24. α-Si_3N_4/β-Si_3N_4 ratio defined by quantitative X-ray diffraction as a function of distance from exterior as-nitrided surface for two dry Si samples and three polymer and solvent exposed samples. Processing histories are summarized in Table 3.

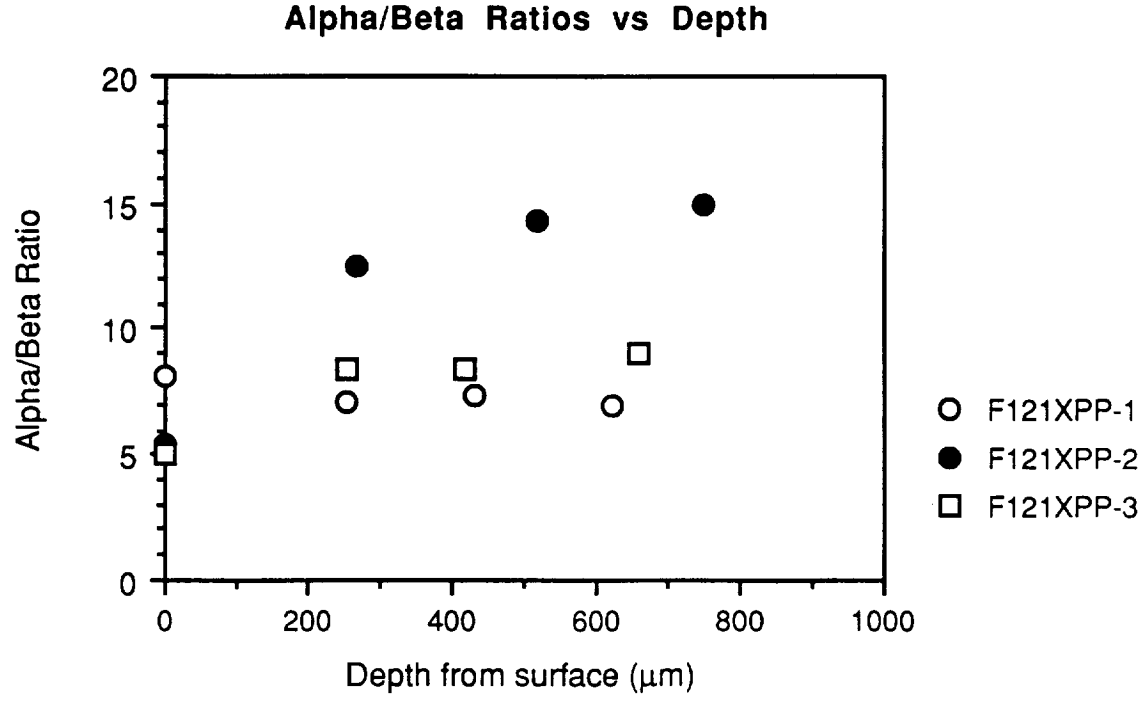

Figure 25. α-Si_3N_4/β-Si_3N_4 ratio defined by quantitative X-ray diffraction as a function of distance from exterior as-nitrided surface for three polymer and solvent exposed samples. Processing histories are summarized in Table 3.

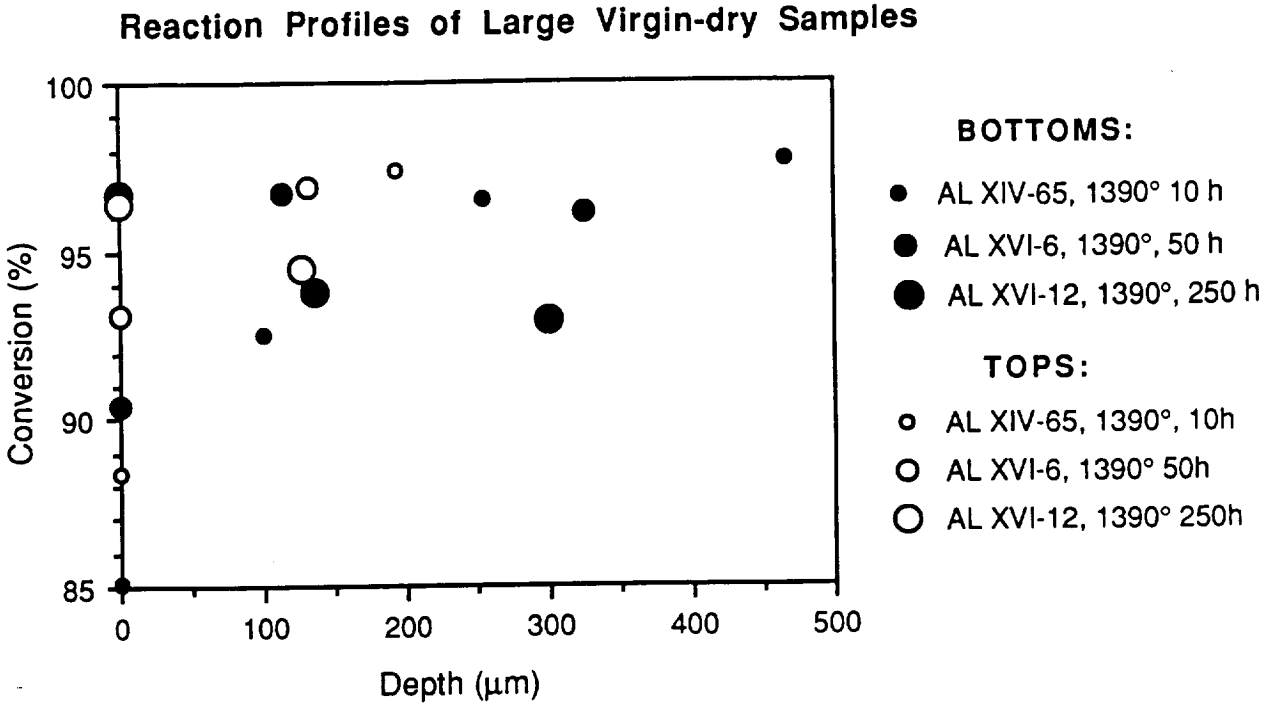

Figure 26. Extent of conversion defined by quantitative X-ray diffraction as a function of distance from exterior as-nitrided top and bottom surfaces for three dry processed, 1" diameter Si samples nitrided by same schedule as sample F121XPS-2.

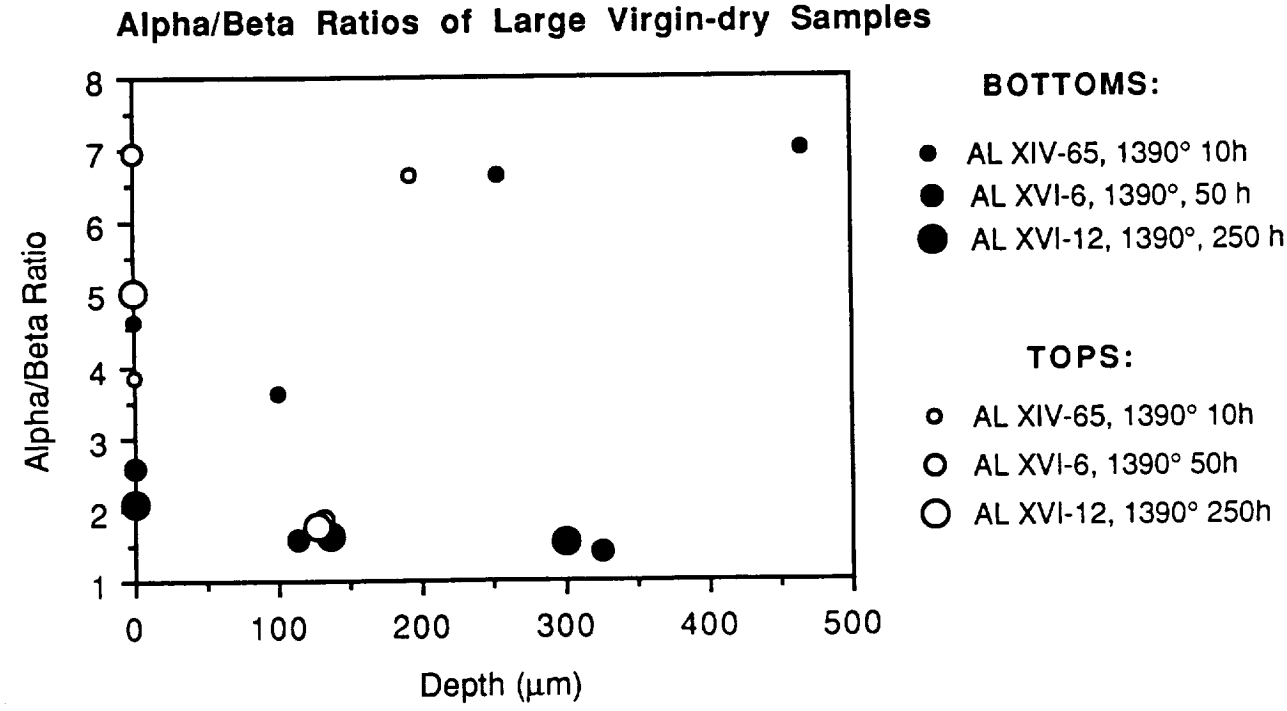

Figure 27. α-Si_3N_4/β-Si_3N_4 ratios defined by quantitative X-ray diffraction as a function of distance from exterior as-nitrided top and bottom surfaces for three dry processed, 1" diameter Si samples nitrided by same schedule as sample F121XPS-2.

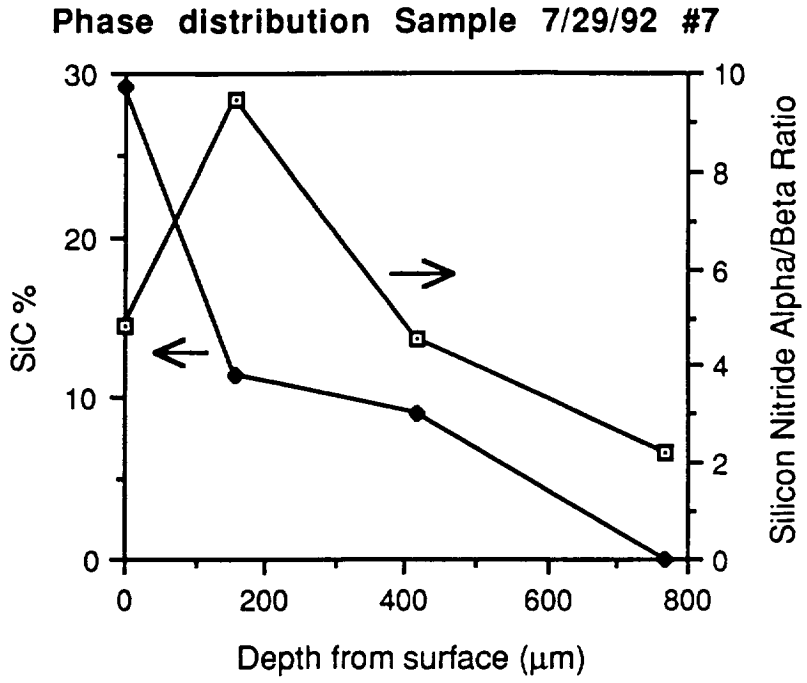

Figure 28. Phase distribution defined by quantitative X-ray diffraction as a function of distance from exterior as-nitrided surface for xylene and polystyrene processed, 1" diameter Si sample nitrided by same schedule as sample F121XPS-2. Sample was located at condensation line outside of hot zone in horizontal tube furnace.

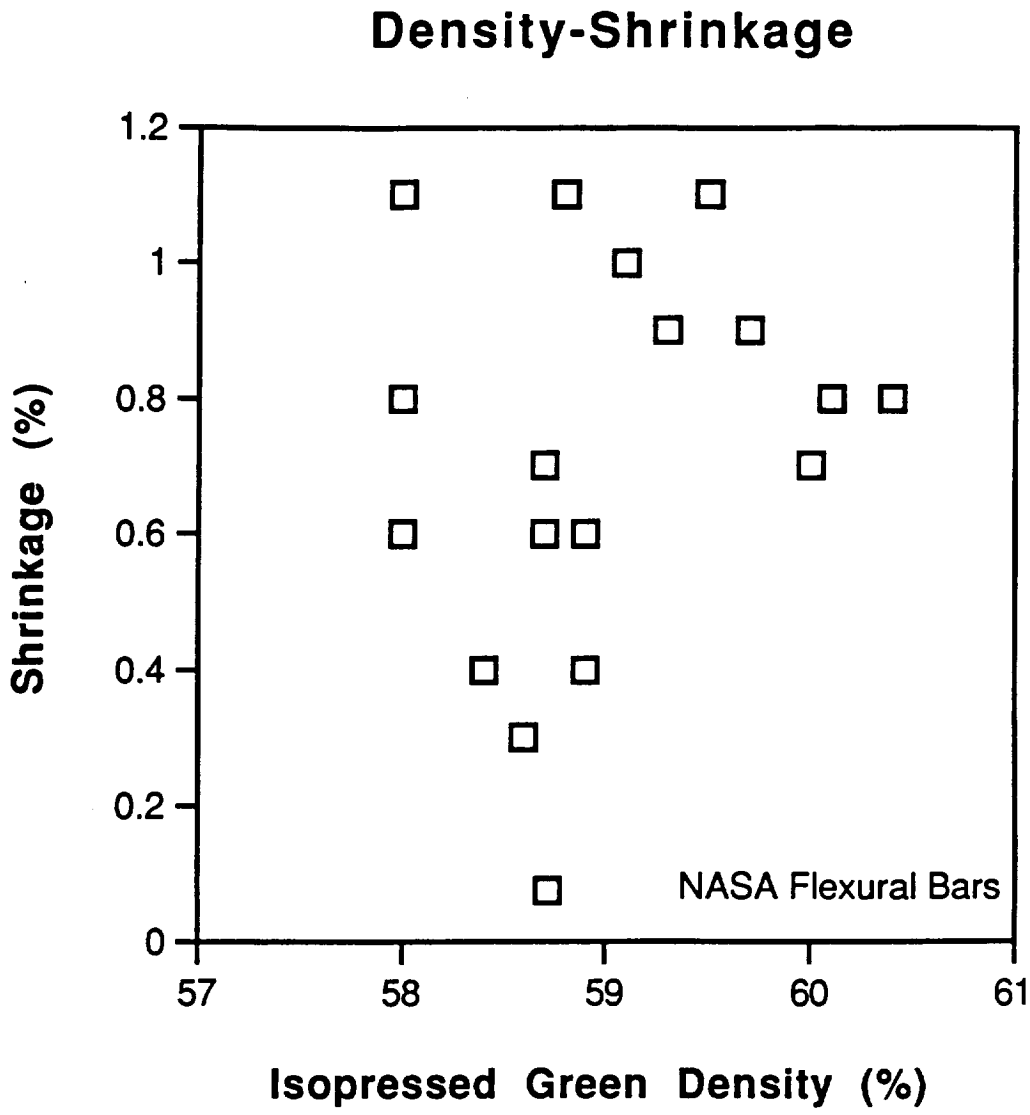

Figure 29. Linear nitriding shrinkages as a function of green, isopressed densities.

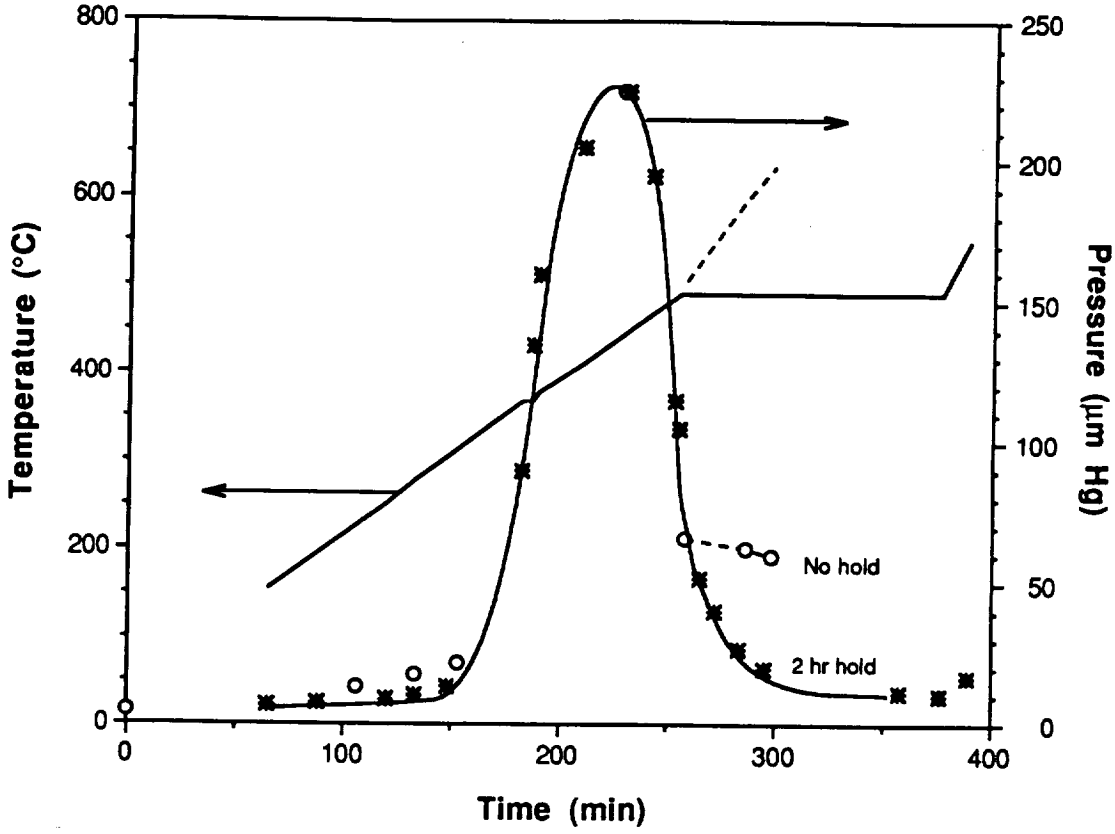

Figure 30. Furnace pressure and temperature profile during vacuum binder removal portion of nitriding schedule C, with and without 2 hr hold at 490°C.